Gut microbiota promotes pain chronicity in Myosin1A deficient male mice

Ana Reynders, Z. Anissa Jhumka, Stéphane Gaillard, Annabelle Mantilleri, Pascale Malapert, Karine Magalon, Anders Etzerodt, Chiara Salio, Sophie Ugolini, Francis Castets, et al.

Brain, Behavior, and Immunity 119 (2024) 750–766

Contents lists available at ScienceDirect

Brain Behavior and Immunity

journal homepage: www.elsevier.com/locate/ybrbi

Gut microbiota promotes pain chronicity in Myosin1A deficient male mice

Ana Reynders [a,1,*], Z. Anissa Jhumka [a,1,2], Stéphane Gaillard [b], Annabelle Mantilleri [a], Pascale Malapert [a], Karine Magalon [a], Anders Etzerodt [c], Chiara Salio [d], Sophie Ugolini [e], Francis Castets [a], Andrew J. Saurin [a], Matteo Serino [f], Guillaume Hoeffel [e], Aziz Moqrich [a,*]

[a] Aix-Marseille-Université, CNRS, Institut de Biologie du Développement de Marseille, Marseille, France
[b] Phenotype Expertise, Marseille, France
[c] Department of Biomedicine, Aarhus University, Aarhus, Denmark
[d] Department of Veterinary Sciences, University of Turin, Grugliasco, TO, Italy
[e] Aix-Marseille-Université, CNRS, INSER, Centre d'Immunologie de Marseille-Luminy, Marseille, France
[f] Institut de Recherche en Santé Digestive, Université de Toulouse-Paul Sabatier, INSERM, INRAe, ENVT, UPS, Toulouse, France

ARTICLE INFO

Keywords:
Chronic pain
Gut microbiota
Dysbiosis
DRG macrophages
Myo1a
Sexual dimorphism
Sex-gene-environmental interactions

ABSTRACT

Chronic pain is a heavily debilitating condition and a huge socio-economic burden, with no efficient treatment. Over the past decade, the gut microbiota has emerged as an important regulator of nervous system's health and disease states. Yet, its contribution to the pathogenesis of chronic somatic pain remains poorly documented. Here, we report that male but not female mice lacking *Myosin1a* (KO) raised under single genotype housing conditions (KO-SGH) are predisposed to develop chronic pain in response to a peripheral tissue injury. We further underscore the potential of MYO1A loss-of-function to alter the composition of the gut microbiota and uncover a functional connection between the vulnerability to chronic pain and the dysbiotic gut microbiota of KO-SGH males. As such, parental antibiotic treatment modifies gut microbiota composition and completely rescues the injury-induced pain chronicity in male KO-SGH offspring. Furthermore, in KO-SGH males, this dysbiosis is accompanied by a transcriptomic activation signature in the dorsal root ganglia (DRG) macrophage compartment, in response to tissue injury. We identify $CD206^{+}CD163^{-}$ and $CD206^{+}CD163^{+}$ as the main subsets of DRG resident macrophages and show that both are long-lived and self-maintained and exhibit the capacity to monitor the vasculature. Consistently, *in vivo* depletion of DRG macrophages rescues KO-SGH males from injury-induced chronic pain underscoring a deleterious role for DRG macrophages in a Myo1a-loss-of function context. Together, our findings reveal gene-sex-microbiota interactions in determining the predisposition to injury-induced chronic pain and point-out DRG macrophages as potential effector cells.

1. Introduction

Pain can be divided into acute and chronic. While acute pain serves a vital protective function, chronic pain reflects a pathological situation, with no protective value. Acute pain occurring after tissue injury is characterized by a transient and reversible hypersensitivity to sensory stimuli, aiming at protecting the injured site from further damage. It results from the sensitization of the components of the pain pathway, including of dorsal root ganglia (DRG) primary sensory neurons (PSNs) and of spinal cord (SC) interneurons, which is initiated by inflammatory mediators released at the injury site (Gangadharan and Kuner, 2013). In contrast, chronic pain manifests through a long-lasting hypersensitivity to sensory stimulations of mechanical and/or thermal nature, with an important impact on the quality of life (Gangadharan and Kuner, 2013; Finnerup et al., 2021). It affects more than 1.5 billion people world-wide and arises as a disease (fibromyalgia), alongside an ongoing disease (chronic osteoarthritis, chemotherapy, diabetes) or following a traumatic event (surgical intervention, nerve injury…) (Borsook, 2012). Several mechanisms are currently acknowledged as drivers of chronic pain states, including maladaptive responses of PSNs and of SC interneurons to tissue injuries (Gangadharan and Kuner, 2013; Finnerup et al., 2021). More recently, immune cells, such as spinal microglia and

* Corresponding authors.
E-mail addresses: ana.reynders@univ-amu.fr (A. Reynders), aziz.moqrich@univ-amu.fr (A. Moqrich).
[1] Authors contributed equally to this study.
[2] Present address: Zuckerman Mind Brain Behavior Institute and Department of Biological Sciences, Columbia University, New York, NY, USA.

https://doi.org/10.1016/j.bbi.2024.05.010
Received 11 August 2023; Received in revised form 23 April 2024; Accepted 3 May 2024
Available online 4 May 2024

DRG macrophages have been also shown to play essential roles in the emergence and maintenance of injury-induced chronic pain states (Hore and Denk, 2019; Guan et al., 2016; Peng et al., 2016; Yu et al., 2020; Ramin Raoof et al., 2021; Zhang et al., 2016). However, in spite of tremendous progress in the understanding of the biology of pain, chronic pain remains a medical challenge, with no efficient long-lasting treatment options (Zimney et al., 2023). This underscores that the knowledge on the mechanisms promoting pain chronicity remains fragmented.

Over the past decades, the commensal organisms that inhabit the gastro-intestinal tract (gut microbiota) have emerged as important regulators of several pain conditions, most of which affect the viscera (O' Mahony et al., 2017; Minerbi and Shen, 2022). For instance, germ-free (GF) animals, which are devoid of gut microbes exhibit higher visceral sensitivity and altered spinal cord gene expression (Luczynski et al., 2017). In addition, patients suffering from irritable bowel syndrome (IBS), bear alterations in the composition of gut microbiota, a situation referred to as gut dysbiosis (Tap et al., 2017). Fecal microbiota transplantations in rodents with samples from human IBS donors is sufficient to induce visceral hypersensitivity, demonstrating that a dysbiotic gut microbiota can cause pain (De Palma et al., 2017). More recently, the gut microbiota has been also implicated in somatic pain conditions (Minerbi and Shen, 2022). In humans, an abnormal composition of the gut microbiota could be associated with chronic post-operative, osteoarthritic pain and fibromyalgia (Yao et al., 2022; Boer et al., 2019; Minerbi et al., 2019; Clos-Garcia et al., 2019). In rodents, GF mice or animals in which the microbiota is depleted by antibiotic administration, develop less sensory hypersensitivity in response to tissue inflammation and to peripheral neuropathies induced by chemotherapy, diabetes and injury of the sciatic nerve (Amaral et al., n.d.; Ding et al., 2021; Ma et al., 2022; Shen et al., 2018). Signalling between the gut microbiota and distant organs occurs by various routes, including endocrine, immune and neural routes, as well as via the production of metabolites derived from the host and gut microbiota (Cryan et al., 2019). Regarding somatic pain conditions, one of the reported mechanisms involves the ability of gut microbiota to modulate immune cells' function. In response to tissue injury, GF mice or mice depleted of gut microbiota, exhibit decreased local production of pro-inflammatory cytokines, decreased macrophage expansion in the DRG, reduced spinal microglial activation and enhanced expansion of regulatory T cells in the spinal cord (Amaral et al., n.d.; Ding et al., 2021; Ma et al., 2022; Shen et al., 2018). Together, these studies show that signals from gut microbiota are required for the initiation of injury-induced sensory hypersensitivity. However, whether and how an abnormal gut microbiota is able to promote pain chronicity remains largely under documented. In the present study, we explore the role of the myosin 1a (MYO1A) protein to injury-induced chronic pain. MYO1A belongs to a large family of atypical type 1 myosins that bridge the cellular membrane to the actin cytoskeleton (McConnell and Tyska, 2010). MYO1A is highly expressed in small intestinal enterocytes where it plays a critical role in microvilli structural organization and subcellular protein trafficking (Tyska et al., 2005a). As such, Myo1a-deficient mice exhibit several impairments related to intestinal function, including perturbations in the trafficking of digestive enzymes, reduced function of the cystic fibrosis transmembrane conductance regulator (CFTR) required for proper mucin secretion and increased sensitivity to dextran sulfate sodium (DSS)-induced colitis (Hegan et al., 2015; Kravtsov et al., 2012; Tyska et al., 2005a). Here, we show that male mice lacking Myo1a (KO) raised under single genotype (KO-SGH) but not under mixed genotype housing conditions (KO-MGH) are predisposed to develop chronic pain in response to a peripheral tissue injury. We further show that this predisposition is linked to alterations in the composition of their gut microbiota. Consistently, parental antibiotic treatment of KO-SGH mice rescues the male offspring from chronic pain and modifies their gut microbiota, highlighting a functional connection between gut microbiota and pain chronicity, in this model. Finally, we propose DRG macrophages as cellular mediators bridging signals from gut microbiota and the emergence of chronic pain in KO-SGH males. Together, our findings reveal gene-sex-microbiota interactions in determining the vulnerability to chronic peripheral pain.

2. Materials and Methods

2.1. Mice

Mice were maintained under standard housing conditions (23 °C, 40 % humidity, 12 h light cycles, and free access to food and water). Special effort was made to minimize the number as well as the stress and suffering of mice used in this study. All experiments were conducted in line with European guidelines for the care and use of laboratory animals (Council Directive 86/609/EEC). All experimental procedures were approved by an independent ethics committee for animal experimentation (APAFIS), as required by the French law and in accordance with the relevant institutional regulations of French legislation on animal experimentation, under license number 34467–20211222154281 v5. *Myo1a* KO mice were generated by Tyska et al., 2005 (Tyska et al., 2005a) and were backcrossed for at least 10 generation on C57BL/6 background (Mazzolini et al., 2013). CX3CR1^{CreERT2} mice were described previously (Yona et al., 2013) and bred with Rosa26-Ai14 mice at the Centre d'Immunologie de Marseille Luminy, as previously described (Hoeffel et al., 2021). Control wild-type (WT) C57BL/6 mice were bred in-house. To generate WT and *Myo1a* KO mice under single genotype housing conditions (WT- and KO-SGH), males and females of each genotype were bred together and the offspring was subsequently analyzed. WT- and KO-SGH founders were separated for at least 4 generations. To generate WT and *Myo1a* KO mice under mixed genotype housing conditions, WT males and *Myo1a* KO females were first bred together allowing to generate F0 heterozygous males and females, which were further bred together and the resulting F1 WT-MGH and KO-MGH mice were housed together after weaning. For the *de novo* generation of WT- and KO-SGH mice, WT-MGH males were bred with WT-MGH females and KO-MGH males were bred with KO-MGH females, and the offspring was analyzed.

To generate pABX-KO-SGH mice, 6 weeks old KO-SGH males and females were provided *ad libidum* with drinking water containing 0.5 g/L ampicillin (Sigma), 0.5 g/L Neomycin (Sigma), 0.5 g/L Metronidazole (Sigma), 0.25 g/L Vancomycin (Sigma) and 3 g/L sucralose for 3 weeks. The antibiotic solution was renewed every other day. One week following antibiotic treatment, crossings were created and the male offspring was subsequently analyzed. The antibiotic-treated crossings were maintained up to the 4th litter and then renewed.

2.2. Tamoxifen administration

A single intra-peritoneal i.p injection of tamoxifen (T5648; 2 mg tam per mouse) at 40 mg/ml in corn oil (C8267; Sigma) was administrated to adult CX3CR1^{CreERT2}:R26-Ai14 mice. Mice were sacrificed at day2, four weeks and twelve weeks post injection. In this model, resident long-lived macrophages will maintain Ai14^{+} fluorescence over time, while circulating monocytes are only Ai14^{+} for several days (Yona et al., 2013). Thus, over time, circulating monocytes (mostly Ai14^{-}) will give rise to monocyte-derived macrophages which will remain Ai14^{-} once seeded into tissues.

2.3. Tracer injections

To identify perivascular macrophages, a single intra-venous (i.v.) injection of dextran-FITC (Thermo, D7136; 5 mg/ml in PBS) was performed. Mice were sacrificed 1 h after injection, intracardially perfused with 10 ml PBS1X and DRG macrophages were analyzed by flow cytometry.

2.4. Histology

To obtain adult Dorsal Root Ganglia (DRGs) specimens for *in situ* hybridization (ISH) and immunostainings, mice were deeply anesthetized with a mix of ketamine/xylazine and then transcardially perfused with an ice-cold solution of paraformaldehyde 4 % in 0.1 M phosphate buffer (4 % PFA). Tissues were further fixed for 24 h in ice-cold 4 % PFA. Newborn P0 mice were sacrificed, rapidly washed in ice-cold PBS, eviscerated and fixed for 24 h in ice-cold 4 % PFA. E15 embryos were collected in ice-cold PBS and fixed for 24 h in ice-cold 4 % PFA. Adult back hairy skin was excised and fixed for 2 h in ice-cold 4 % PFA. Specimens were transferred into a 30 % (w/v) sucrose solution for cryoprotection before being frozen in OCT mounting medium. 12 μm cryosections (DRGs) and 18–20 μm cryosections (SC, skin, E15 and P0) were obtained using a standard cryostat (Leica).

2.5. In situ hybridization

Dioxigenin-labeled *Myo1a* antisense probe and Fluorescein-labeled *TrkB* probe were synthetized using gene-specific PCR primers and cDNA templates from adult mouse DRG and ISH or double ISH was carried as described in Reynders et al., 2015(Reynders et al., 2015). The primers used for probe synthesis are listed below.

Myo1a F1: GAAAATACTTCCGGTCAGGTG
Myo1a R1: CAAGGGTTCTTCATCTCTGAGT
Myo1a F2: TACCAGTGGAAGTGCAAGAAGT
Myo1a R2 + T7: TAATACGACTCACTATAGGGACACTACGAAGTTCT GCTCCAG
TrkB-F1: CTGAGAGGGCCAGTCACTTC,
TrkB-R1: CATGGCAGGTCAACAAGCTA,
TrkB-F2: CAGTGGGTCTCAGCACAGAA,
TrkB-R2 + T7: TAATACGACTCACTATAGGGCTAGGACCAGGATGG CTCTG

2.6. Immunostaining

Immunostainings were done with rat anti-GINIP (1:500, Moqrich laboratory), goat anti-Ret (1:500, R&D Systems), rabbit anti-TrkA (1:1000, generous gift from Dr. L. Reichardt, University of California), goat anti-TrkC (1:500, R&D Systems), rabbit anti-CGRP (1:1000, ImmunoStar), rabbit anti-PKCγ (1:500, Santa Cruz), rabbit anti- PGP9.5 (1:200, Thermo Scientific) and rabbit-anti S100 (1:1000, Darko). IB4 labelling was performed with Alexa Fluor 488-conjugated IB4 from Invitrogen. Slides were mounted with ImmuMount (Thermo Scientific) prior to observation under AxioImager Z1 (Zeiss) fluorescence microscope. Contrast was adjusted using Photoshop software.

For SC and skin innervation, image acquisition was performed using an LSM-780 confocal microscope (Zeiss) and same pinhole aperture, lasers intensities as well as gain parameters were respected between WT and KO specimens.

2.7. Cell counts

Total and subsets of DRG neurons were counted on lumbar L4 DRG from adult WT and *Myo1a* KO mice, as described in Gaillard et al., 2014 (Gaillard et al., 2014). Briefly, 12 μm serial sections of L4 DRG were distributed on 6 slides which were subjected to different markers, including the pan-neuronal marker PGP9.5. This approach allowed us to refer all counting to the total number of neurons (PGP9.5). For each genotype, three independent experiments were performed.

2.8. Behavioral tests

All behavioral analyses were conducted on 8–12 weeks old KO and WT males and females. All experiments were carried at room temperature (~22 °C). Animals were acclimated for one hour to their testing environment prior to all experiments. Experimenters were blind to the genotype of the mice during testing. The number of tested animals is indicated in the figure legends section.

2.8.1. Openfield, rotarod and hot plate

tests were carried as described in Gaillard et al(Gaillard et al., 2014).

2.8.2. Acetone test

Acetone drop evaporation assay(Hulse et al., 2012) was used to assess naïve mice's sensitivity to innocuous skin cooling. A drop of acetone was applied on the left hind paw using a 1 ml syringe. The duration of flinching/pain like behavior (seconds) was recorded immediately following acetone application for a total period of 2 min. The test was repeated twice and the mean duration of flinching/pain behavior was calculated.

2.8.3. Heat hypersensitivity

Hind paw heat hypersensitivity was determined prior and at different time-points (see legend Extended Data Fig. 4) after paw incision surgery, using Hargreaves plantar test, as described in Gaillard et al., 2014(Gaillard et al., 2014).

2.8.4. Mechanical thresholds

Mechanical thresholds of the plantar surface were determined using Von Frey filaments with the up-down method(Chaplan et al., 1994), previously as described(Gaillard et al., 2014) prior to and at several time-points after inflammation, neuropathy and paw-incision surgery, as indicated in the corresponding figure legends.

2.9. Injury-induced pain models

2.9.1. Zymosan-A induced inflammation

20 μL of a solution containing 0.06 mg Zymosan-A in 0.9 % NaCl (weight/vol, Sigma), were injected subcutaneously into the plantar side of the left hindpaw, using a 30G needled syringe(Witschi et al., 2011).

2.9.2. Chronic constriction injury (CCI)

Unilateral peripheral mono-neuropathy was induced in ketamin/xylasin-anesthetized mice by performing two loosely tied ligatures (with about 1 mm spacing) around the common sciatic nerve(Bennett and Xie, 1988) using monocryl resorbable suture filaments (6–0, Ethicon, Piscataway, NJ, USA). The nerve was constricted to a barely discernable degree, so that circulation through the epineurial vasculature was not interrupted. After surgery, the animals were allowed to recover in a warming chamber, and then they were returned to their home cages.

2.9.3. Paw incision

The paw incision pain model was performed as described by Brennan et al. 1999(Brennan, 2004). Briefly, mice were anesthetised with ketamin/xylasin and a 5 mm longitudinal incision of the plantar face of the right hindpaw, starting from 2-5 mm from the proximal edge of the heel was performed. The plantar muscle was then carefully elevated with forceps and incised longitudinally with a blade, while leaving muscle's origins intact. The wound was closed with one horizontal mattress suture using 6.0 silk monofilament (Ethicon, Piscataway, NJ, USA) and the wound site was covered with betadin ointment. After surgery, the animals were allowed to recover in a warming chamber, and then they were returned to their home cages.

2.10. Taxonomic and predicted functional analysis of gut microbiota

Feces were collected from individual naïve mice in an Eppendorf tube and immediately frozen on dry ice. The collection was performed between 11AM and 1PM on mice from at least 3 different cages and 2

different crossings. Total DNA was extracted from feces as already reported (Serino et al., 2012). The 16S rRNA gene V3-V4 regions were targeted by the 357wf-785R primers and analysed by MiSeq at RTLGenomics (Texas, USA). An average of 16,564 sequences per mouse was generated for WT-SGH and KO-SGH mice of each sex presented in Fig. 2b-e and Extended Data Fig. 5; an average of 62,880 sequences per mouse was generated for WT-MGH and KO-MGH males in Fig. 2g-h; an average of 55,455 sequences per mouse was generated for KO-SGH and pABX-KO-SGH males presented in Fig. 3d-f. Cladograms in were drawn by using the Huttenhower Galaxy web application *via* LEfSe(Segata et al., 2011). Principal component analyses (PCA) and Operational Taxonomic Unit (OUT)-based diversity indices were determined with the software PAST4.10.

2.11. RNA extraction

Mice were deeply anesthetized with a mix of ketamine/xylazine and transcardially perfused with 5–10 mL RNA Later (Quiagen). L3 to L4 DRGs were rapidly dissected and RNA was extracted by using RNeasy Micro Kit (Quiagen), according to manufacturer's instructions. For quality control, RNAs were loaded on an RNA PanoChip (Agilent) and processed with 2100 Bioanalyzer system (Agilent technology).

2.12. High-throughput RNA sequencing and analyses

WT-SGH, KO-SGH and pABX-KO-SGH DRG RNAs were extracted in experimental triplicates from individual mice. High quality RNA (RIN > 8.5) was used for sequencing. RNA-seq libraries were prepared using the TruSeq RNA Sample Preparation Kit (Illumina). All libraries were validated for concentration and fragment size using Agilent DNA1000 chips. Sequencing was performed on a HiSeq 2000 (Illumina), base calling performed using RTA (Illumina) and quality control performed using FastQC (https://www.bioinformatics.bbsrc.ac.uk/projects/fastqc) and RSeQC(Wang et al., 2012). Sequences were uniquely mapped to the mm10 genome using Subread(Liao et al., 2013) (C version 1.4.6-p2) using default values. Reads mapping to gene exons (GRCm38.p4 gene assembly) were counted using featureCounts(Liao et al., 2014) (C version 1.4.6-p2). Differential gene expression was performed using exon counts from biological replicates using the DESeq2 BioConductor R package(Love et al., 2014), using a 1 % false discovery rate (FDR) and log2 Fold Change of 0.5 cutoff. Heat-maps and K-means clustering with one minus Pearson correlation were generated using Morpheus on-line software (https://software.broadinstitute.org/morpheus). Functional analysis was performed using Metascape software (Zhou et al., 2019).

WT-SGH, KO-SGH and pABX-KO-SGH, CCI vs naïve differentially-expressed genes (DEG) are depicted in Supplementary Tables 1, 2 and 3, respectively.

KO-SGH versus WT-SGH, pABX-KO-SGH versus KO-SGH and pABX-KO-SGH versus WT-SGH DEG at day 60 post CCI can be found in Supplementary Tables S4-S6, respectively.

2.13. qRT-PCR

RNA obtained from each sample was converted into cDNA using Superscript III Reverse Transcriptase (Invitrogen). Gene expression was assessed by quantitative PCR (qPCR), using qPCR Sybr-Green master mix (ThermoFisher). Samples were run for 40 cycles on a StepOne qPCR apparatus (Applied Biosystems). The relative quantity of transcripts was determined by normalization to *Gapdh* using the standard ΔCt method.

The primers sequences used for qPCR are:

Myo1a F: CTACGAGCAGCTTCCCATCT
Myo1a R: CCACATTTGCCAAAGCATAG
Gapdh F: ATGGTGAAGGTCGGTGTGA
Gapdh R: AATCTCCACTTTGCCACTGC

2.14. Flow cytometry on DRG and SC cell suspensions

DRG cells suspensions for flow cytometry analysis were prepared as previously described, with minor modifications (Reynders et al., 2015). Mice were deeply anesthetized with a mix of ketamine/xylazine with 10 ml of PBS1X, via intra-cardiac injection. Ipsilateral and contralateral L3 to L5 DRGs were dissected in ice-cold HBSS-glucose (HBSS1X (Gibco) supplemented with 100 mM D-glucose (Sigma), 50 mM HEPES (Gibco), 100 U/ml Penicillin and 100 μg/ml Streptomycin (Gibco), pH 7.4) and were incubated for 50 min at 37 °C with a mixture of 2 mg/ml collagenase II (Gibco), 5 mg/ml dispase (Gibco) and 40 μg/ml DNAseI (Roche) diluted in HBSS-glucose supplemented with 3 mM CaCl2. At the end of the incubation time, the enzyme-containing medium was carefully removed without disturbing the DRGs and was replaced with fresh ice-cold HBSS-glucose. DRGs were mechanically dissociated by gentle trituration performed with a P1000 pipet.

SC was carefully removed from the vertebral column and the meninges and dorsal roots were peeled-off. SC tissue was cut into small pieces before being digested using a mixture of collagenase D (2 mg/ml, Roche), DNAseI (50 μg/ml, Roche), diluted in RPMI medium (Gibco), for 1 h at 37 °C. At the end of the enzymatic digestion, SC pieces were immediately placed on ice, supplemented with ice-cold RPMI + 10 % FCS and triturated using 21-G needles-equipped syringes. The resulting cell suspensions were filtered on 100 μm filters, washed with RPMI + 10 %FCS and centrifugated at 1500 rpm, 4 °C, for 7 min.

DRG and SC cell suspensions were centrifuged for 10 min at 1500 rpm, 4 °C and were further processed for flow cytometry immunostaining. DRGs cell suspensions were incubated with Mouse BD Fc Block™ (clone 2.4G2, BD bioscience), diluted in FACS buffer (PBS1X supplemented with 0.5 % BSA (Sigma) and 2 mM EDTA (Gibco)) for 15 min on ice, then they were stained with a mix of fluorophores-labelled antibodies, for 50 min on ice. After washing with FACS buffer, then with PBS1X, death cells were stained using LIVE/DEADTM Fixable Aquadead Cell Stain Kit for 405 nm excitation (Invitrogen) according to manufacturer's instructions. Cells were fixed using the Foxp3/Transcription Factor Fixation/Permeabilization Concentrate and Diluent Kit (eBioscience), according to manufacturer's instructions. Stained cells were analyzed on an LSR-Fortessa X20 cytometer (BD bioscience) and FlowJo software was used for data analysis.

The antibody mix contained: rat anti-mouse CD206-AlexaFluor488 or CD206-APC (1:300, clone C068C2, BioLegend), rat anti-mouse CD163-PE or CD163-APC (1:500, clone S15049F, BioLegend), Ly6G-APC-Cy7 (1:400, clone1A8, BioLegend), rat anti-mouse Ly6C-BV421 (1:400, clone AL-21, BD bioscience), CD11b-BV510 (1:1000, clone M1/70, BD bioscience), rat anti-mouse IA-IE-AlexaFluor700 (1:500, clone M5/114.15.2, BioLegend), rat-anti mouse CD64-BV711 (1:300, clone X54-5/7.1, Biolegend), rat-anti mouse CD45-BV785 (clone 30F-11, Biolegend), armenian hamster anti-mouse CD11c-BUV385 (1:200, clone N418, BD Biosciences) and rat anti-mouse CD24-BUV737 (1:500, clone M1/69, BD Bioscience).

2.15. PLX5622 administration

PLX5622 was purchased from DC chemicals (DC21518). A solution of PLX5622 at a concentration of 0.008 mg/μl was obtained by dissolving the PLX5622 powder in DMSO (10 %) supplemented with corn oil (90 %). The vehicle was prepared equally, but does not contain PLX5622.

To test the depletion efficiency of DRG macrophages and to monitor SC microglia, two series of five consecutive intraperitoneal injections (injection 1: day 1 PM; injection 2: day 2 AM; injection 3: day 2 PM; injection 4: day 3 AM; injection 5: day 3 PM, see Fig. 6) with 10 μL/g (corresponding to 0.08 mg/g) of the PLX5622 solution or the vehicle was performed either in naïve WT- and KO-SGH mice.

For behavioral analysis, two series of five consecutive injections with PLX5622 or its vehicle were performed in KO-SGH males starting from

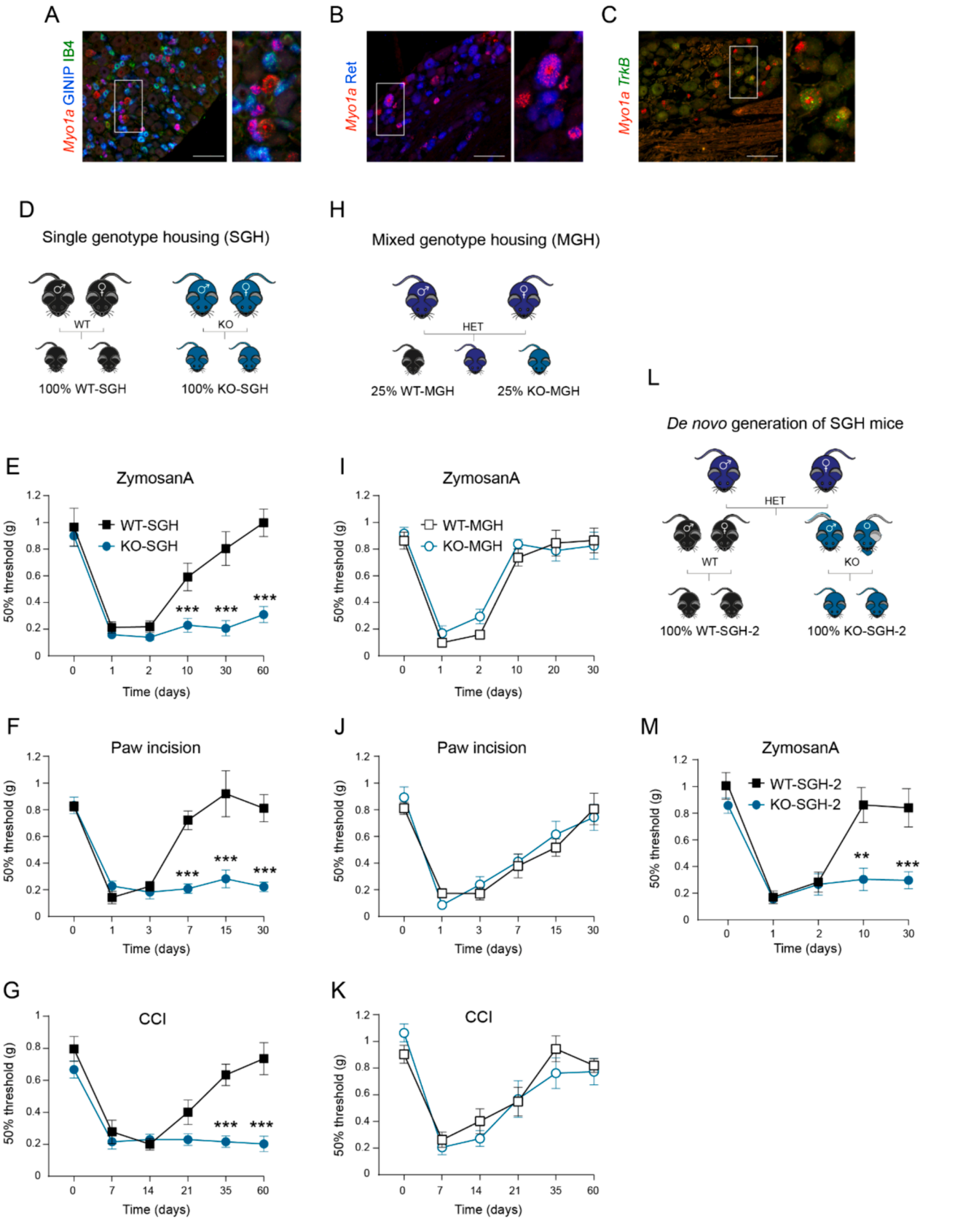

(caption on next page)

Fig. 1. Myo1a-deficient male mice raised under single genotype but not mixed genotype housing conditions exhibit a predisposition to injury-induced mechanical pain. **A-C**, In situ hybridization (ISH) showing the expression of *Myo1a* (red) in adult lumbar DRG neurons. **A**, co-labelling with anti-GINIP (blue) and IB4 (green). **B**, co-immunolabelling with anti-Ret (blue). **C**, double ISH with *TrkB* (green) probe. Scale bars 100 μm **D**, Schematic representation of breeding and housing of WT and KO mice raised under single genotype housing (SGH) conditions. **E-G** Mechanical thresholds of WT-SGH and KO-SGH males in response to tissue injuries induced by Zymosan A, n = 9 per genotype (**E**), paw-incision, n = 10 per genotype (**F**) and chronic constriction injury (CCI), n = 9 wt-SGH and 10 KO-SGH (**G**). **H**, Schematic representation of breeding and housing of WT and KO mice raised under mixed genotype housing conditions (MGH). **I-K**, Mechanical thresholds of WT-MGH and KO-MGH males in response to tissue injuries induced by Zymosan A, n = 9 per genotype (**I**), paw-incision, n = 12 wt-SGH and 11 KO-SGH (**J**) and by CCI, n = 8 per genotype (**K**). **L**, Schematic representation of the experimental design allowing the de novo generation of WT-SGH-2 and KO-SGH-2 mice from MGH founders. **M**, Mechanical thresholds of WT-SGH-2 (n = 11) and KO-SGH-2 (n = 14) males in response to Zymosan A. Data are presented as mean ± SEM for each group. ***P < 0.01, Two-Way Repeated Measures ANOVA followed by Bonerroni's multiple comparisons test. (For interpretation of the references to colour in this figure legend, the reader is referred to the web version of this article.)

day 7 after paw incision surgery (first series: between days 7 and 9 post paw incision; second series: between days 14 and 16 post paw incision, see Fig. 7).

2.16. Statistical analyses

The n numbers of individuals or experimental replicates and the statistical test are indicated in the corresponding figure legend. Statistical analyses were performed with Prism software.

3. Results

3.1. Myo1a-deficient males raised under single genotype housing conditions exhibit a vulnerability to injury-induced chronic pain

In a previous study, in which we analysed the transcriptional signature of flow-cytometry activated cell-(FAC-) sorted C-Low-Threshold Mechanoreceptors (C-LTMRs), followed by an extensive *in situ* hybridisation validation, we showed that C-LTMRs share a common gene expression profile with other subsets of LTMRs, including Aδ- and Aβ fibers (Reynders et al., 2015). LTMRs innervate the skin, from where they convey innocuous mechanical stimuli under physiological conditions, and they also participate to injury-induced mechanical hypersensitivity (Abraira and Ginty, 2013; Delfini et al., 2013; Xu et al., 2015). Within the common LTMRs set of genes, we identified *Myo1a* as being highly enriched in Gαi-Inhibitory Interacting Protein (GINIP)-positive Isolectin Binding 4 (IB4)-negative C-LTMRs, as expected, but also in Tropomyosin receptor kinase B (*TrkB*)-expressing Aδ LTMRs and in large-diameter Aβ-LTMRs expressing the tyrosine kinase receptor Ret (Fig. 1A-C). In DRGs, *Myo1a* was detectable at embryonic day 15 (E15) in a small subset of large-diameter neurons and its expression extended at birth to the majority of DRG neurons (Fig.S1A-B). In adult mice, *Myo1a* was restricted to LTMRs, as it was undetectable in peptidergic TrkA-positive, non-peptidergic IB4-positive and proprioceptive TrkC-expressing neurons (Fig. S1C-E). In addition, *Myo1a*-encoding transcripts were undetectable in the adult SC by qRT-PCR, or in brain areas such as hippocampus and cerebellum (Fig. S1F).

MYO1A caught our attention because it is closely related to MYO1C which is critical for inner ear hair cell mechano-transduction (Stauffer et al., 2005). On this basis, we sought to investigate the function of MYO1A in somato-sensory biology, by analyzing *Myo1a* Knock-Out (KO) mice (Tyska et al., 2005b). As these mice were available as homozygous breeders and because they were on a pure C57Bl/6J background (Mazzolini et al., 2013), we initiated our study by comparing *Myo1a*-KO mice to control C57Bl/6J wild type (WT) mice, which were generated from homozygous crosses. Under these conditions, *Myo1a*-KO and WT mice evolved in single-genotype housing conditions (hereafter respectively called KO-SGH and WT-SGH) (Fig. 1D). Global analysis of KO-SGH mice showed that MYO1A is dispensable for the survival, molecular maturation and target innervation of PSNs, including those that normally express *Myo1a* (Fig. S2).

Additionally, KO-SGH and WT-SGH mice had similar behaviour in the open filed and rotarod tests (Fig. S3A-B). They exhibited no difference in their ability to sense noxious heat and cold stimuli, as shown by their responsiveness in the hot plate and in the acetone tests (Fig. S3C-D).

Because *Myo1a* is expressed in LTMRs, we tested the mechanical sensitivity of KO-SGH and WT-SGH male mice at steady-state and at different time-points following tissue injury elicited by intra-plantar administration of Zymosan A (Witschi et al., 2011), paw incision surgery (Brennan, 2004) and chronic constriction injury (CCI) of the sciatic nerve (Bennett and Xie, 1988). By using the up-and-down method of the Von Frey test, we showed that male mice of both genotypes had similar baseline mechanical thresholds and developed significant and similar mechanical hypersensitivity in all three paradigms (Fig. 1E-G). However, in contrast to WT-SGH males in which the injury-induced mechanical hypersensitivity progressively resolved over time, KO-SGH males exhibited persistent mechanical hypersensitivity in all three pain models (Fig. 1E-G). Notably, in the CCI model, while WT-SGH males recovered their baseline mechanical threshold 45 days post-injury, KO-SGH males remained hypersensitive up to 180 days (6 months) post-CCI (Fig. S4A). Interestingly, and in line with the selective expression of Myo1a in LTMRs, paw incision-induced thermal hyperalgesia was similar between KO-SGH and WT-SGH mice (Fig. S4B). Furthermore, in contrast to KO-SGH males, KO-SGH females did not exhibit persistent mechanical hypersensitivity in response to Zymosan A-, paw incision- and CCI-induced injuries (Fig. S5A-C). These data demonstrate that KO-SGH males exhibit a vulnerability to injury-induced chronic pain. They further show that the loss of MYO1A facilitates the transition from acute to chronic injury-induced pain in a sex-dependent manner. Knowing the importance of the interaction between the host and the microbial genomes in determining a given phenotype (Stappenbeck and Virgin, 2016), we asked whether MYO1A loss-of-function (LOF) *per se* was sufficient to explain our observed phenotype. Towards this aim, we generated WT and KO littermates, evolving in mixed genotype housing conditions (hereafter called WT-MGH and KO-MGH respectively) (Fig. 1H). Under these housing conditions, KO-MGH mice exhibited the same mechanical thresholds as their WT-MGH littermates in response to intra-plantar Zymosan A injection, paw-incision surgery and CCI (Fig. 1I-K). Both groups of mice developed similar injury-induced mechanical hypersensitivity and, in sharp contrast with KO-SGH males, both KO-MGH and WT-MGH exhibited a full recovery of the mechanical sensitivity from tissue injury (Fig. 1I-K). From these data, we conclude that MYO1A genetic deletion *per se* is insufficient to explain the establishment of the chronic pain phenotype in KO-SGH males. However, these results strongly suggest that environmental factors related to MYO1A loss of function may contribute to promoting injury-induced pain chronicity in KO-SGH males. Consistent with this hypothesis, *de novo* generation of KO-SGH and WT-SGH second generation male mice from MGH-KO and MGH-WT founders, recapitulates the chronic pain phenotype following intra-plantar injection of Zymosan-A (Fig. 1L-M). Together these data demonstrate that gene-environment interactions are required to trigger the vulnerability to injury-induced chronic pain in myosin 1a-deficient male mice.

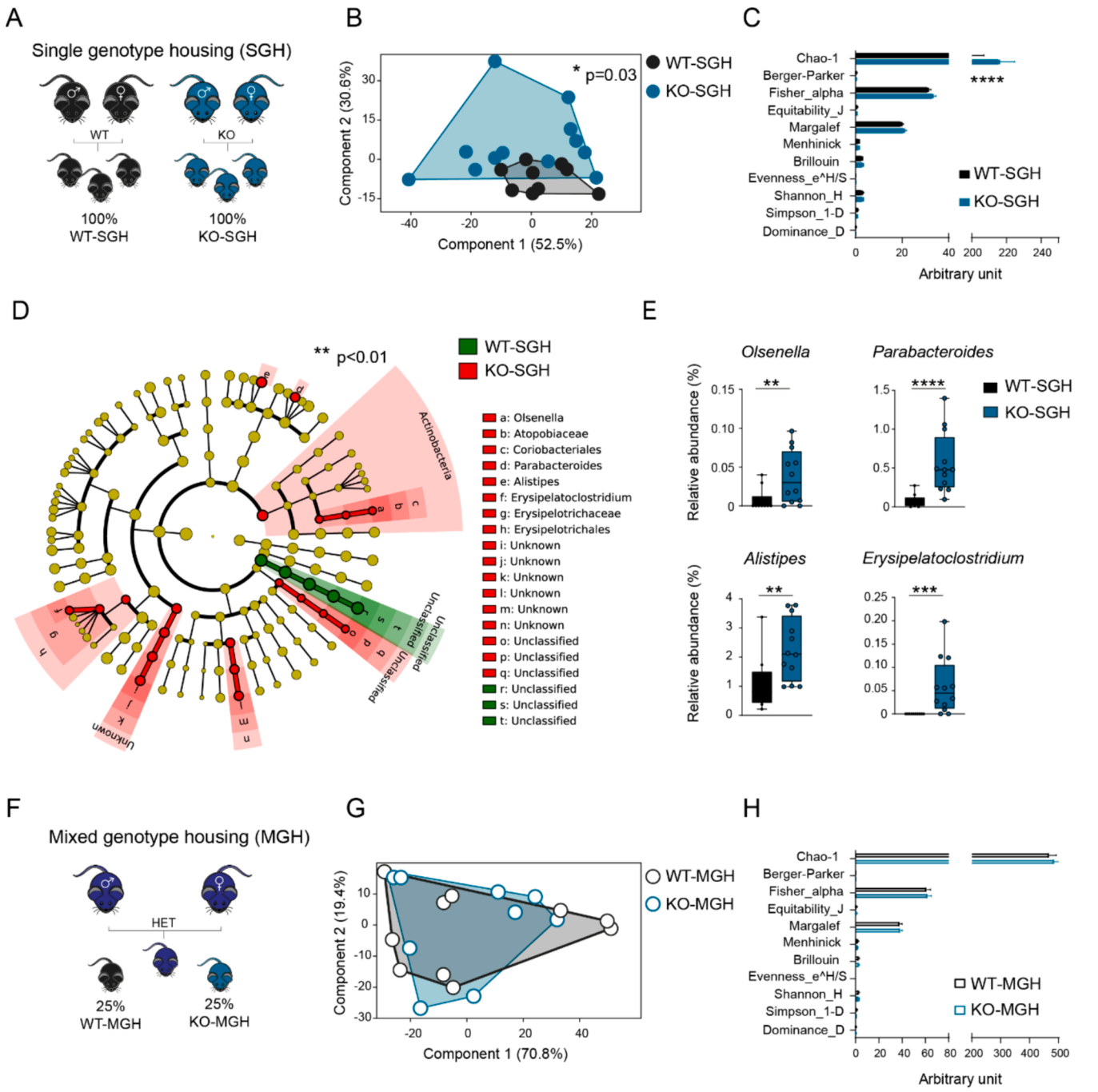

Fig. 2. KO-SGH but not KO-MGH males exhibit alterations in the gut microbiota composition. **A**, Schematic representation of breeding and housing of WT-SGH and KO-SGH mice. **B**, Principal component analysis (PCA) of gut microbiota of WT-SGH (n = 10) and KO-SGH (n = 12) males, $^{*}P < 0.05$, 1-way PERMANOVA with Bonferroni correction. **C**, Diversity indices of gut microbiota of WT-SGH and KO-SGH males, $^{****}P < 0.0001$, 2-way ANOVA followed by a 2-stage linear step-up procedure of Benjamini, Krieger and Yekutieli to correct for multiple comparisons by controlling the False Discovery Rate (<0.05). **D**, Cladogram showing bacterial taxa significantly higher in WT-SGH and KO-SGH gut microbiota (the cladogram shows taxonomic levels represented by rings with phyla at the innermost and genera at the outermost ring and each circle is a bacterial member within that level). **E**, Relative abundance of *Olsenella*, *Parabacteroides*, *Alistipes* and *Erysipelatoclostridium* in WT-SGH and KO-SGH gut microbiota, $^{**}P < 0.01$, $^{***}P < 0.001$, $^{****}P < 0.0001$, Mann Whitney *U* test. **F**, Schematic representation of breeding and housing of WT-MGH and KO-MGH mice. **G**, Principal component analysis (PCA) of gut microbiota of WT-MGH and KO-MGH males. **H**, Diversity indices of gut microbiota of WT-MGH and KO-MGH males.

3.2. KO-SGH but not KO-MGH male mice exhibit strong alteration in the gut microbiota composition

Knowing that the absence of MYO1A in the small intestine leads to impaired structure and function of intestinal epithelial cells (Hegan et al., 2015; Kravtsov et al., 2012; McConnell et al., 2009; Tyska et al., 2005b), we hypothesised that the predisposition of KO-SGH males to develop chronic mechanical pain may be related to an altered gut microbiota. To test this hypothesis, we first performed 16S rRNA gene sequencing from faecal samples of WT and KO male mice raised under SGH and MGH conditions. Principal Component Analysis (PCA) of diversity indices and Linear Discriminant Analysis (LDA) for effect size

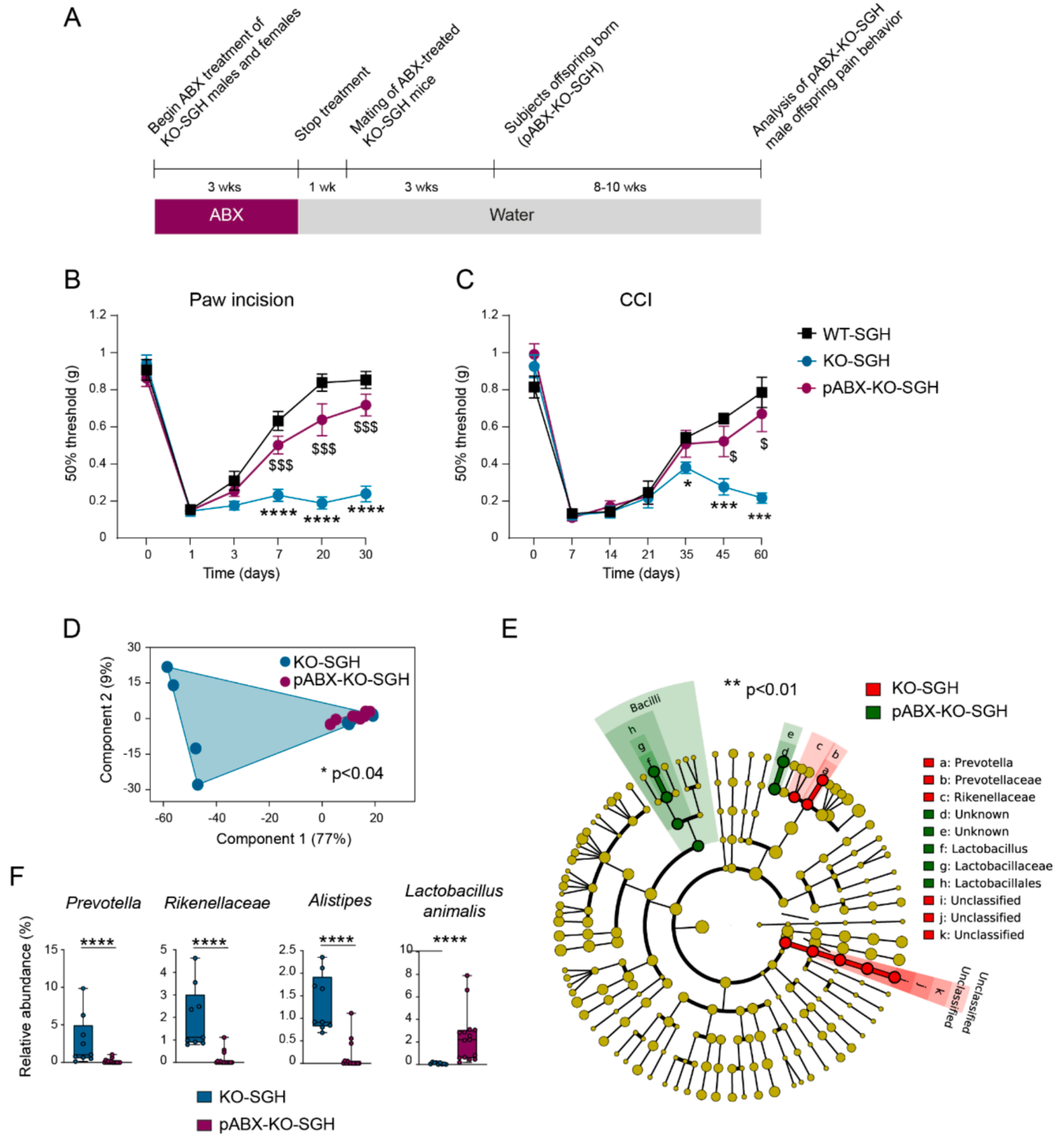

Fig. 3. Antibiotic treatment of KO-SGH parents rescues the male offspring from chronic pain. A, Experimental design for antibiotic administration to KO-SGH males and females before breeding and subsequent analysis of pABX-KO-SGH male offspring. **B-C**, Mechanical thresholds of indicated mice following paw incision, n = 19 wt-SGH, 17 KO-SGH and 21 pABX-KO-SGH and CCI, n = 7 wt-SGH, 8 KO-SGH and 7 pABX-KO-SGH (**C**). Mixed effect analysis using Restricted Maximum Likelihood Model and Tukey's post-hoc test; KO-SGH vs WT-SGH: $^{*}P < 0.05$, $^{***}P < 0.001$, $^{****}P < 0.0001$, KO-SGH vs pABX-KO-SGH: $\$P < 0.05$, $\$P < 0.001$, WT-SGH vs pABX-KO-SGH: non-significant. **D**, Principal component analysis (PCA) of gut microbiota of KO-SGH (n = 9) and pABX-KO-SGH males (n = 15), $^{*}P < 0.05$, 1-way PERMANOVA with Bonferroni correction. **E**, Cladogram showing bacterial taxa significantly higher in KO-SGH and pABX-KO-SGH gut microbiota. **F**, Relative abundance of *Prevotella*, *Rikenellaceae*, *Alistipes* and *Lactobacillus animalis* in KO-SGH and pABX-KO-SGH gut microbiota, $^{***}P < 0.001$, $^{****}P < 0.0001$, Mann Whitney *U* test.

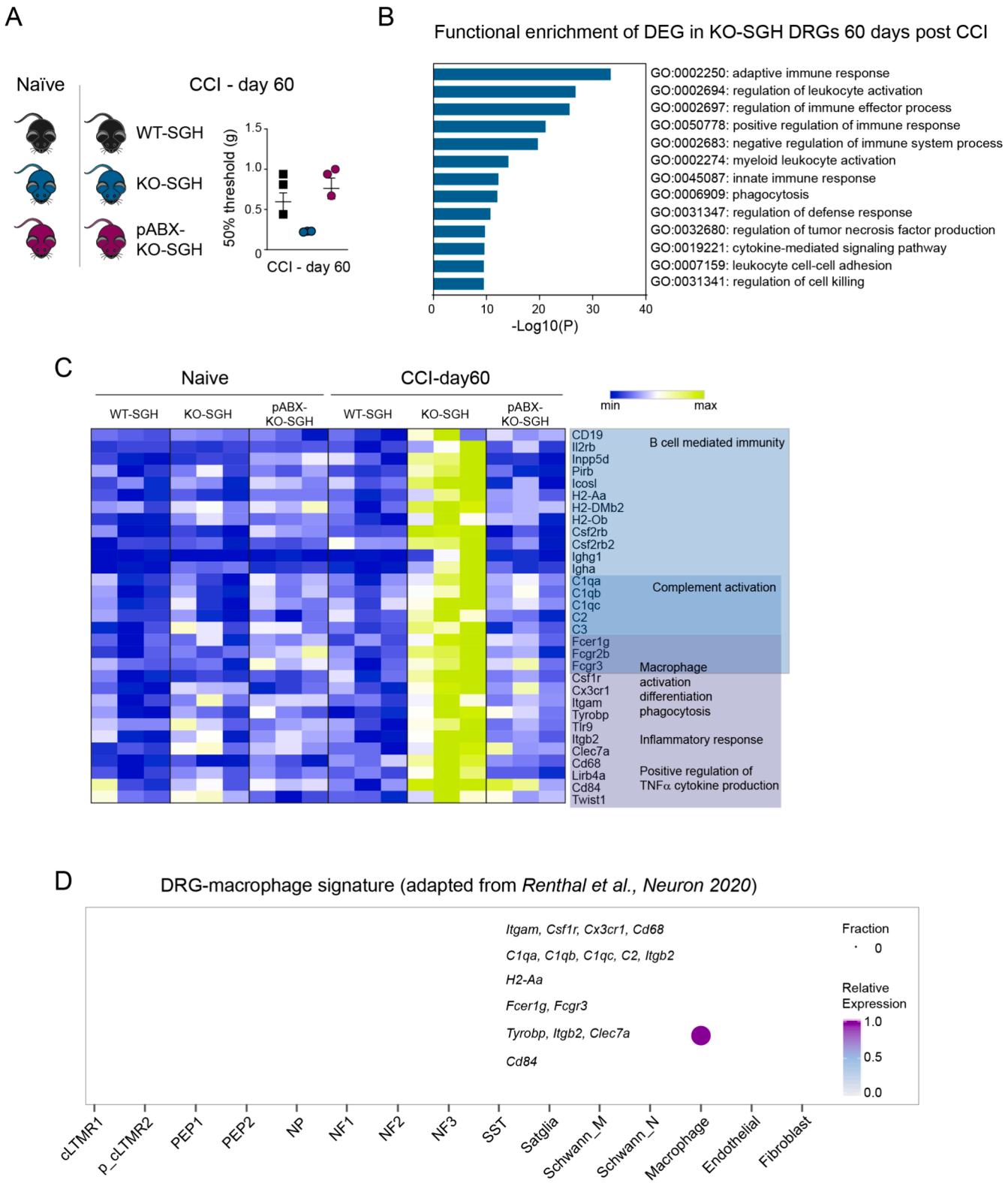

Fig. 4. CCI induces a sustained transcriptional macrophage signature in the DRGs of KO-SGH, which is rescued by parental antibiotic treatment. A, Shows the experimental design and the mechanical threshold of the individuals used for RNA-Seq at 60 days post-CCI (n = 3/genotype/condition). B, Gene Ontology (GO) terms enriched in the sets of up-regulated genes in KO-SGH DRGs at 60 days post-CCI. C, Heat-map representing the expression levels (Transcripts Per Million) of indicated genes in naïve and CCI-day 60 DRGs from WT-SGH (n = 3), KO-SGH (n = 3) and pABX-KO-SGH (n = 3) males. Shows the biological processes in which these genes are involved, as determined by GO analysis. D, Shows the expression of the indicated genes across the distinct DRG cellular types identified in the snRNA-Seq database from (Renthal et al., 2020).

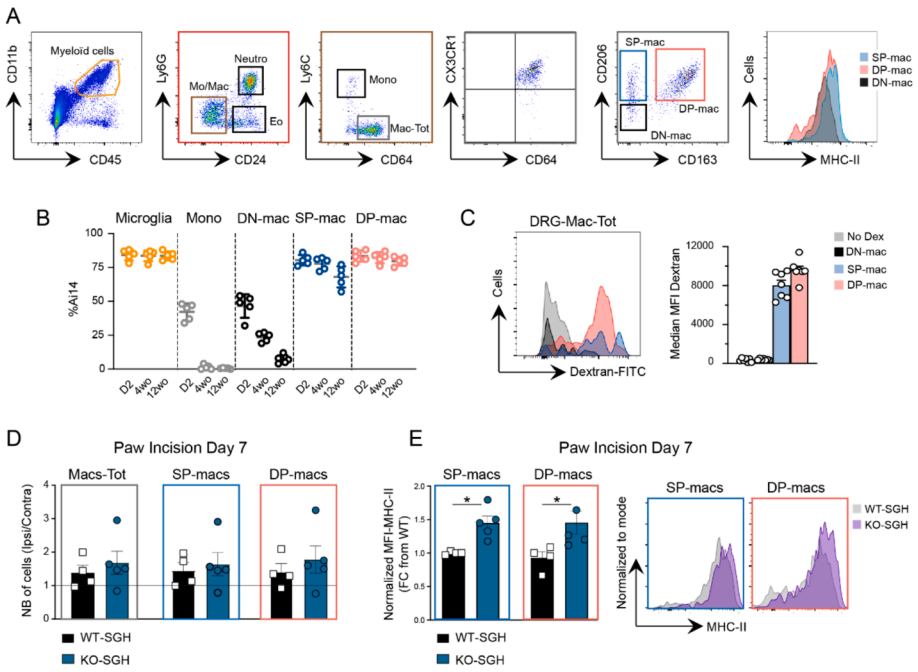

Fig. 5. Enhanced activation of DRG macrophages subsets following paw-incision, in KO-SGH males. A, Shows the gating strategy for the identification of DRG myeloid cell subsets with flow cytometry. CD11b^{+}CD45^{+} live cells are subdivided into Ly6G^{+}CD24^{+} Neutrophils (Neutro), Ly6G-CD24^{+} Eosinophils (Eo) and Ly6G^{-}CD24^{-} cells containing Monocytes and Macrophages (Mo/Mac). The Mo/Mac subset is divided into Ly6C^{hi}CD64^{-} Monocytes (Mono) and Ly6C^{-}CD64^{+} Macrophages (Mac-Tot) that co-express CX3CR1. The Mac-Tot subset is further subdivided into CD206^{+}CD163^{-} (SP-mac), CD206^{+}CD163^{+} (DP-mac) and CD206^{-}CD163^{-} (DN-mac). DN-macs (grey) exhibit lower levels of MHC-II than SP-(blue) and DP-macs (red). **B**, Shows the percentage of Ai14-expressing cells in spinal microglia, circulating blood monocytes (Mono), and DN-, SP- and DP-mac subsets of DRG macrophages at day 2 (D2), 4 and 12 weeks (4wo and 12 wo) after a single administration of tamoxifen (TAM) in adult CX3CR1$^{CreERT2:R26\text{-}Ai14}$ mice (see also Materials and Methods), n = 5 individuals per time/point. **C**, (Left) Flow cytometry histogram showing Dextran-FITC (500 KDa) uptake by DN-, SP- and DP-mac subsets in the DRG and (Right) the quantification of the median fluorescence intensity (MFI) for Dextran-FITC in each subset (n = 5–6 individuals/time-point). **D**, Shows the ipsilateral:contralateral ratio of the absolute numbers (NB) of Mac-Tot, SP-macs and DP-mac the DRGs of WT-SGH (n = 4) and KO-SGH (n = 5) males, at day 7 post paw-incision. **E**, Shows the variations in the MHC-II median fluorescence intensity normalized to mode (MFI) in SP- and DP-mac DRG subsets of WT-SGH (n = 4) and KO-SGH (n = 5), expressed as fold-change (FC) from the mean of WT-SGH ipsilateral DRGs. The right histograms are representative profiles of the normalized MHC-II expression in the ipsilateral DRGs of WT-SGH (grey) and KO-SGH (purple) males. Note the right-shift in KO-SGH, representative of a higher MHC-II expression. *$P < 0.05$, Mann Whitney U test. (For interpretation of the references to colour in this figure legend, the reader is referred to the web version of this article.)

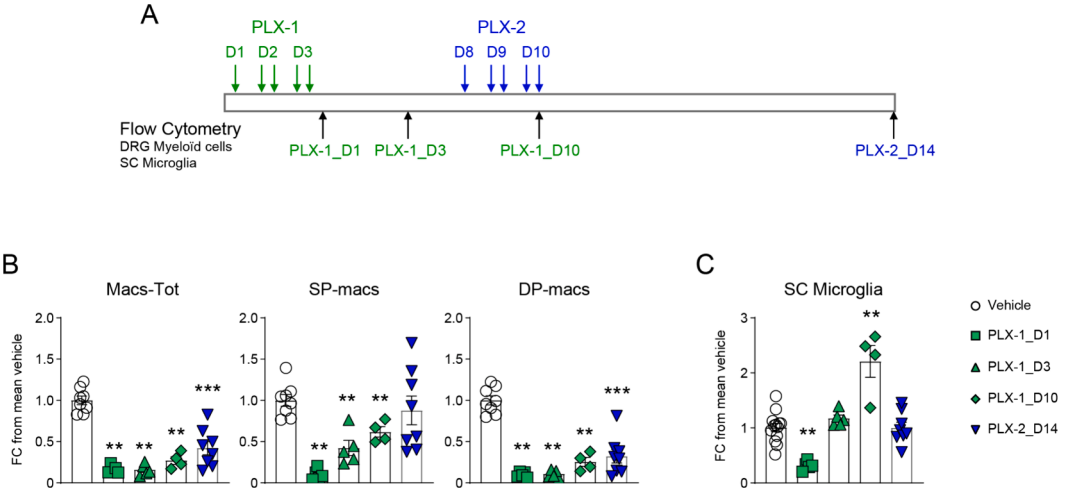

Fig. 6. PLX5622 administration induces a robust and sustained depletion of DP-macs subset in the DRGs. A, Experimental design for PLX5622 (PLX) administration and the selected time-points for subsequent analysis of DRG macrophages and spinal cord (SC) microglia with flow cytometry. **B-C**, Shows the relative numbers of total DRG macrophages (Macs-Tot), SP-macs and DP-macs subsets (**in B**) and spinal microglia (**in C**) in vehicle (n = 8), PLX-1_D1 (n = 4), PLX-1_D3 (n = 5), PLX-1_D10 (n = 4) and PLX-2_D14 (n = 8) conditions expressed as the fold change (FC) from the mean value of vehicle condition. Spinal microglia were gated as live cells CD11b^{+}CD45^{low}. **P < 0.01, *** P < 0.001, Mann Whitney U test.

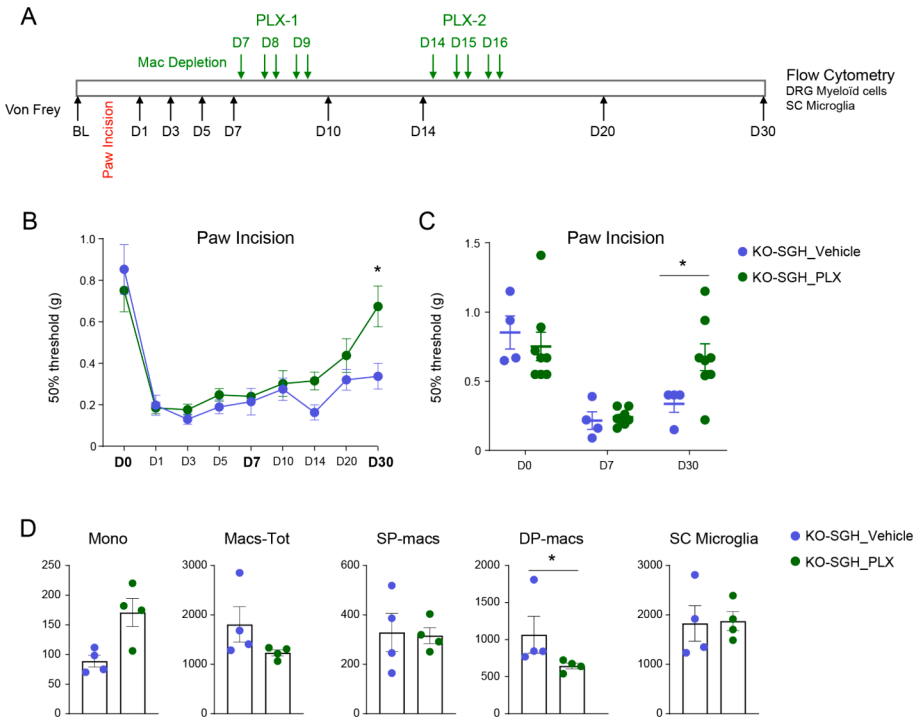

Fig. 7. ***In vivo*** **macrophage depletion rescues KO-SGH males from injury-induced chronic pain. A**, Experimental design for PLX5622 (PLX) administration in the paw-incision model. **B-C**, Mechanical thresholds of vehicle (n = 4) and PLX-treated (n = 8) KO-SGH males following paw incision. *$P < 0.05$, Mixed effect analysis using Restricted Maximum Likelihood Model and Bonferroni's post-hoc test; KO-SGH_Vehicle vs KO-SGH_PLX. **D**, Shows the absolute numbers of Mono, Mac-Tot, SP-mac and DP-mac subsets in the ipsilateral DRGs and of spinal microglia, determined with flow cytometry in KO-SGH_Vehicle (n = 4) and KO-SGH_PLX (n = 4) mice, at day 30 post paw incision. Spinal microglia were gated as live cells $CD11b^{+}CD45^{low}$. *$P < 0.05$, Mann Whitney *U* test.

(LEfSe) revealed a shift in gut microbiota composition of KO-SGH males compared to the WT-SGH counterparts (Fig. 2A-E). This shift was due to an increase in the abundance of rare taxa in KO-SGH, as shown by the Chao-1 index, though the overall diversity was unchanged between groups (Fig. 2C). KO-SGH male mice had a higher relative abundance of Olsenella, *Parabacteroides, Alistipes and Erysipelatoclostridium* (Fig. 2D-E), previously associated with a disease state such as periodontitis for *Olsenellea* (Gómez-García et al., 2022), neurodegenerative disorders and/or depression for *Parabacteroides* and *Alistipes* (Bonnechère et al., 2022) and high fat diet for *Erysipelatoclostridium* (Tomas et al., 2016). In contrast, we found no significant difference in the gut microbiota composition of KO-MGH males as compared to their WT-MGH littermates (Fig. 2F-H). This is in line with previous studies reporting a normalisation of gut microbiota between genotypes, when mice are raised as littermates (Robertson et al., 2019). We also found that KO-SGH females exhibited alterations in their gut microbiota composition as compared to WT-SGH females, despite being protected from injury-induced chronic pain (Fig. S5D-G). This shift was due to increased abundance in rare taxa, such as *Olsenella*, *Parabacteroides distasonis* and *Canidiatus Athromitus* (Fig. S5F-G). Comparison of female versus male gut microbiota in KO-SGH and WT-SGH animals suggests a dominant contribution of the genotype in determining the composition of gut microbiota (Fig. S6). However, sex-related differences were observable in the abundance of certain taxons as well as in the functional output (Fig. S6). The gut microbiota of KO-SGH females was enriched in Lactobacillales probiotic species (*L.animalis* and *L.reuteri*) (Fig. S6B-C). Interestingly Lactobacillales were more abundant also in WT-SGH females as compared to males, suggesting a female-preferential expansion of this taxon in our vivarium (Fig. S6F-G).

Altogether our data underscore the potential of MYO1A loss of function to shape the composition of the gut microbiota.

3.3. Antibiotic treatment of KO-SGH parents rescues male offspring from chronic pain

Our results uncover a link between the dysbiotic gut microbiota and the vulnerability to injury-induced chronic pain of KO-SGH male mice. To test this, we decided to deplete the gut microbiota of KO-SGH parents and to analyse the underlying consequences on their male offspring. Such experimental design takes into consideration the maternal contribution in shaping the offspring gut microbiota (Buffington et al., 2016; Goodrich et al., 2014; McCafferty et al., 2013). It also considers possible paternal horizontal transmission, as in our animal facility, both parents are housed with their pups. KO-SGH males and females of six weeks of age were treated with a cocktail of large spectrum antibiotics (ABX) for three weeks (Shen et al., 2018), whereupon the treatment was stopped and ABX-KO-SGH breeding pairs were formed (Fig. 3A). We analysed the response of adult male offspring (hereafter named pABX-KO-SGH) to paw incision and CCI as well as their gut microbiota composition (Fig. 3B-C). In both pain models, pABX-KO-SGH male mice were compared to KO-SGH and WT-SGH. While all three groups developed similar paw incision- and CCI-induced mechanical hypersensitivity (Fig. 3B-C), KO-SGH mice remained hypersensitive at day 30 in the paw incision model and at day 60 in the CCI model. Importantly, in both pain models, pABX-KO-SGH male mice exhibited the same kinetics of recovery as the WT-SGH mice, further supporting the idea that the dysbiotic microbiota in KO-SGH males participates to their vulnerability to injury-induced pain (Fig. 3B-C). Consistently, following 16S rRNA gene sequencing analyses of faecal samples, PCA and LEfSe revealed a significant shift in the gut microbiota composition of pABX-KO-SGH males compared to SGH-KO males (Fig. 3D-F). In particular, pABX-KO-SGH mice had a statistically significant lower relative abundance of bacteria such as *Prevotella*, *Alistipes* and *Rikenellaceae* and higher relative abundance of bacteria from class Bacilli, such as Lactobacillus, including

Lactobacillus animalis, a probiotic species with beneficial properties (Chen et al., 2022) (Fig. 3E-F). Overall, these data uncover the potential of the gut microbiota in influencing the vulnerability to chronic pain, in KO-SGH males.

3.4. Tissue injury induces a sustained transcriptional signature in the DRG of KO-SGH males which is rescued by parental antibiotic treatment

To understand the mechanisms promoting pain chronicity in KO-SGH males, we performed RNA deep sequencing of ipsilateral DRG of adult WT-SGH, KO-SGH and pABX-KO-SGH males under naïve conditions and at day 60 post-CCI (Fig. 4A). Analysis of CCI versus naïve differentially expressed genes (DEG) within the same group and subsequent functional analysis, highlighted differences in the pathways recruited in response to CCI between WT-SGH, KO-SGH and pABX-KO-SGH (Fig. S7 and Supplemental Tables S1-S3). Since at day 60 post-CCI WT-SGH and pABX-SGH-KO males fully recovered normal mechano-sensitivity while KO-SGH males remained hypersensitive (see Fig. 3C), we sought to identify the sets of differentially-expressed genes (DEG) only in the KO-SGH CCI-day60 condition. These particular groups of DEG likely reflect those that are associated with pain persistency in KO-SGH males and which are sensitive to regulation by gut-microbiota derived signals. Using, multiplex comparison combined with K-means clustering, we identified a set of 137 DEG up regulated preferentially in KO-SGH post-CCI (Fig. S8 and Supplemental Tables S4-S6). Metascape functional analyses (Zhou et al., 2019) revealed a prominent enrichment in genes involved in the immune response (Fig. 4B-C). These included genes involved in adaptive immune response, inflammatory response and positive regulation of cytokine production, demonstrating that several immune effector functions are enhanced in the DRGs of KO-SGH post-CCI (Fig. 4B-C). Strikingly, interrogation of the DRG snRNA-Seq database provided by Renthal and colleagues (Renthal et al., 2020) revealed a cluster of transcripts exclusively expressed in DRG macrophages (Fig. 4D). These included signature genes such as the CD11b-encoding gene *Itgam*, widely expressed on myeloid cells, the Colony Stimulating Factor Receptor 1 *Csf1r*, the chemokine receptor *Cx3cr1* and *Cd68*, reminiscent of macrophages recruitment, survival and activation. Several other genes reflected a possible enhanced activation of DRG macrophages such as transcripts encoding the Major Histocompatibility Complex II proteins (*H2-Aa* and *H2-Eb1*), activating and inhibitory Fc receptors (*Fcer1g* and *Fcgr3*), and proteins associated with the complement system (*C1qa*, *C1qb*, *C1qc*, *C4b, Itgam, Itgb2*). In addition, this macrophage cluster also contained the Pathogen Recognition Receptor *Clec7a*, highly expressed in phagocytic macrophages and in pathogenic microglia (Shi et al., 2022; Wang et al., 2022), including in neuropathic-pain promoting microglia (Wu et al., 2022) and the DAP-12 encoding gene *Tyrobp,* also up-regulated in pathogenic microglia and necessary for the induction of neuropathic pain (Guan et al., 2016; Zhang et al., 2013). Together, these data underscore a sustained and/or enhanced activity of DRG macrophages that could contribute to the pain chronicity observed in KO-SGH males.

3.5. In vivo macrophage depletion rescues KO-SGH males from injury-induced chronic pain

Macrophages are immune cells endowed with high plasticity that fulfil a wide-range of functions, including host-defence, inflammation control and tissue repair (Vannella and Wynn, 2017; Hoeffel et al., 2021). DRG macrophages expand in response to peripheral injuries (Yu et al., 2020; Ramin Raoof et al., 2021; Zhang et al., 2016; Cobos et al., 2018; Van Der Vlist et al., 2022; Singh et al., 2022; Feng et al., 2023; Liang et al., 2020) and they have the ability to either support tissue healing (Van Der Vlist et al., 2022; Singh et al., 2022; Feng et al., 2023) and inflammatory pain resolution or to perpetuate pain chronicity (Yu et al., 2020; Ramin Raoof et al., 2021; Zhang et al., 2016). However, despite recent studies, the ontogeny, diversity, turn-over and function of DRG macrophages in response to a peripheral insult remains elusive (Feng et al., 2023; Lund et al., 2024). We used flow cytometry to characterize and monitor the DRG macrophage compartment, at steady state and following paw-incision (Fig. 5). We used a panel of antibodies that allowed us to monitor DRG immune cells of myeloid origin ($CD45^+CD11b^+$), which contain neutrophils ($Ly6G^+CD24^+$) and other granulocytes, likely eosinophils ($Ly6G^-CD24^+$) as well as monocytes and macrophages (Fig. 5A). In the $Ly6G^-CD24^-$ gate, monocytes were identified as $Ly6C^{hi}$ expressing cells, while macrophages were $Ly6C^-CD64^+$ cells that homogenously expressed CX3CR1 (Fig. 5A, right part). These $CD64^+$ macrophages could be further subdivided into 3 subsets based on the combinatorial expression of the mannose receptor CD206, widely expressed on tissue-resident macrophages and of the scavenger receptor CD163, mainly expressed on perivascular macrophages (Fig. 5A, right part). We thus identified a subset of $CD206^+CD163^+$ double-positive macrophages (DP-macs) as the major population (60 ± 1.69 %) of DRG macrophages, consistent with a recent report (Lund et al., 2024). We also observed a subset of $CD206^+CD163^-$ simple positive macrophages (SP-macs, 27.9 ± 0.75 %) as well as a small subset of $CD206^-CD163^-$ double negative macrophages (DN-macs, 4.7 ± 0.55 %). These were largely dominated by MHC-II-expressing macrophages, but DN-macs expressed lower levels of MHC-II (Fig. 5A, right part). To determine the self-maintenance capacity of DRG macrophages, we performed tracing experiments using the $CX3CR1^{CreERT2:R26\text{-}Ai14}$ system (Hoeffel et al., 2021; Yona et al., 2013). Tamoxifen (TAM) administration to adult $CX3CR1^{CreERT2:R26\text{-}Ai14}$ mice labeled microglia for up to 12 weeks but monocytes were only labeled for 2 days (Fig. 5B). The analysis of DN-, SP- and DP-macs in DRGs revealed that both SP- and DP-macs remained highly labelled up to 12 weeks, but SP-macs were less efficiently labelled at 4 and then 12 weeks after TAM injection reminiscent to their monocyte dependency (Fig. 5B). This demonstrate that SP- and DP-macs are long-lived macrophages with high self-maintenance capacities (Hoeffel et al., 2015). In sharp contrast, the Ai14 expression in DN-macs rapidly declined, showing that this subset is monocyte-derived (Fig. 5B). To evaluate the relationship of these three subsets of macrophages with the fenestrae vascular system of DRGs (Jimenez-Andrade et al., 2008; Lund et al., 2024), we also analyzed their capacity to uptake circulating dextran (500 kDa) (Fig. 5C). One hour after injection, flow cytometry analysis showed that, in clear contrast to the DN subset, SP- and DP-macs were efficiently capturing circulating Dextran, revealing their perivascular nature. Together these data imply that SP- and DP-macs are long-lived cells that may be primed in the early life by circulating factors, including metabolites released by the gut microbiota.

We next determined the numbers of total macrophages and SP-macs and DP-macs in the ipsilateral and contralateral L3-L5 DRGs of WT-SGH and KO-SGH males at day 60 following. CCI. In both genotypes, we observed a two-fold increase in the number of SP- and DP-macs in the ipsilateral DRGs, showing that the expansion of DRG macrophages after a CCI injury can persist beyond the recovery from the injury-induced mechanical hypersensitivity (Fig. S9). Similarly, at day 7 following paw-incision surgery, we observed an equivalent accumulation of SP- and DP-mac subsets in the ipsilateral versus contralateral DRGs, in both WT-SGH and KO-SGH males (Fig. 5D). However, in KO-SGH males, both SP- and DP-mac subsets expressed higher levels of MHC-II, suggesting an enhanced activation of DRG macrophages (Fig. 5E).

Functionally speaking, because these data do not exclude that DRG macrophages may promote chronic pain in KO-SGH males, we designed an *in vivo* depletion protocol, which consists of two series of intraperitoneal injections of PLX5622 (a CSF1R antagonist, hereafter referred to as PLX-1 for the first series of injections and PLX-2 for the second one) or its vehicle (Fig. 6A). Flow cytometry analysis of DRG macrophages subsets and of SC microglia was performed at days 1, 3 and 10 post PLX-1 and at day 14 post PLX-2 (Fig. 6B-C). At day 1 post PLX-1, SP and DP subsets of DRG macrophages were robustly depleted as well as SC microglia (Fig. 6B-C). The SP subset was progressively replenished at day 3, reached higher levels at day 10 post PLX-1 before returning to

baseline levels at day 14 post PLX-2 (Fig. 6B). Similarly, SC microglia reached control numbers at day 3 post PLX-1 and expanded at day 10 post PLX-1 (Fig. 6C). Importantly, at day 14 post PLX-2 the numbers of SC microglia were no longer impaired (Fig. 6C). In contrast, the depletion was sustained for the DP-mac subset up to day 10 after PLX-1 and also at day 14 after PLX-2 (Fig. 6B). Therefore, our PLX protocol is designed to ensure a robust depletion of SP- and DP- subsets of DRG macrophages.

We thus applied this PLX protocol to KO-SGH males, in our paw incision model, starting from day 7 post-surgery and we subsequently monitored the mechanical sensitivity over time and the numbers of DRG monocytes, macrophages and the SC microglia, at the end of the experiment (Fig. 7A). Remarkably, behavioral analysis showed that PLX-treated KO-SGH males were rescued from paw incision-induced chronic pain, as they recovered their baseline mechanical threshold at day 30, while the vehicle-treated group remained hypersensitive, at this time point (Fig. 7B-C). Flow cytometry analysis of DRG macrophages performed on 4 mice per condition, showed a significant reduction in the numbers of DP-mac in the ipsilateral L3-L5 DRGs of PLX-treated KO-SGH males at day 30 (Fig. 7D). Of note, there was a tendency for an increase in monocyte numbers in PLX-treated subjects, however spinal microglia were unaffected (Fig. 7D). Together, these data highlight the ability of DRG macrophages to mediate injury-induced chronic pain in KO-SGH males.

4. Discussion

In this study, we uncover the potential of gut microbiota to influence the vulnerability to injury-induced chronic somatic pain, in Myosin 1a knock-out male mice. The extent to which the gut microbiota impacts somatic pain remains poorly established. Recent studies on the topic carried out in non-genetically manipulated mouse models have underscored the ability of gut microbiota to prevent or decrease the onset of neuropathic pain induced by nerve injury, chemotherapy or diabetes and to participate to pain perpetuation (Chen et al., 2021; Ding et al., 2021; Ma et al., 2022; Shen et al., 2018). Human clinical studies also provide evidence for a contribution of gut microbiota to the intensity and chronicity of post-operative pain (Brenner et al., 2021; Yao et al., 2022). We depict here gene-microbiota interactions in the settlement of chronic somatic pain, in Myo1a-deficient males. We found that KO-SGH non-littermates but not KO-MGH littermates males exhibited a predisposition to chronic injury-induced mechanical pain, that was accompanied by a dysbiotic microbiota. *De novo* generation of KO-SGH males from KO-MGH littermate founders recapitulated the vulnerability to chronic mechanical pain, demonstrating that MYO1A loss of function generates a detrimental environment promoting the vulnerability to chronic mechanical pain. Consistently, perturbation of gut microbiota in KO-SGH parents by antibiotic administration completely reversed the pain chronicity in their pABX-KO-SGH male offspring and promoted the expansion of beneficial bacteria such as *Lactobacillus animalis* (Chen et al., 2022).

The extent to which host genotype affects the composition of gut microbiota remains highly debated. While littermate controls are considered as the gold standard to unambiguously demonstrate the contribution of a genetic mutation to a given phenotype, they reach limitations when a phenotype is also driven by the gut microbiota (Robertson et al., 2019; Stappenbeck and Virgin, 2016; Viennois et al., 2020). Indeed, MGH conditions standardise the composition of gut microbiota across genotypes by normalising the maternal transmission and the horizontal transfer between mice of the same cage (Robertson et al., 2019). Accordingly, depending on the type of mutation, littermate separation after weaning and/or homozygous crosses over one or more generations are needed to allow a genetic mutation to impact on the gut microbiota (Elinav et al., 2011; Fulde et al., 2018; Lemire et al., 2017; Mamantopoulos et al., 2017; Viennois et al., 2020). In our experimental paradigm, KO-SGH males were derived from KO-SGH parents; they acquire their gut microbiota from KO-SGH females, which are also dysbiotic and are housed only with KO mates over several generations, favouring the emergence of gene-related shifts in microbiota composition (Viennois et al., 2020). In addition, prenatal antibiotic treatment persistently affects the gut microbiota in male KO-SGH offspring, further suggesting that once the microbiota is perturbed, several generations may be necessary in order to re-establish the initial microbiota (Viennois et al., 2020). Therefore, our data highlight the potential of MYO1A loss of function to shape the composition of gut microbiota. This is further supported by the fact that MYO1A is highly expressed in intestinal epithelial cells and that the absence of MYO1A leads to cellular defects that may interfere with gut microbiota composition (Hegan et al., 2015; Kravtsov et al., 2012; McConnell et al., 2009; Tyska et al., 2005b). As such Myo1a-deficient mice exhibit perturbations in the trafficking of CFTR resulting in diminished CFTR function (Kravtsov et al., 2012). CFTR is essential for mucus production and decreased CFTR function has been reported in models of high-fat-diet induced dysbiosis (Gustafsson et al., 2012; Tomas et al., 2016). Moreover, Myo1a-deficient mice exhibit defaults in the generation of enterocyte-derived luminal vesicles (McConnell et al., 2009). Luminal vesicles released from the enterocytes contain high concentrations of alkaline phosphatase which limit the expansion of luminal bacteria (Shifrin et al., 2012). Finally, Myo1a-deficient mice are more sensitive to DSS-induced colitis, further arguing that the absence of intestinal MYO1A may disrupt the intestinal barrier (Hegan et al., 2015).

Mechanistically, we found that dysbiosis of gut microbiota was associated with perturbations and/or enhanced activity of DRG macrophages in response to tissue injury. RNA-sequencing analyses revealed that 60 days post-CCI, the DRGs of KO-SGH males but not WT-SGH exhibited the transcriptional hallmarks of an activated state of DRG macrophages, which was rescued by parental antibiotic treatment. Consistent with our findings, previous studies reported that the protection from injury-induced sensory hypersensitivity by antibiotic-mediated microbiota depletion can be achieved by decreasing the inflammatory response mediated by DRG macrophages (Shen et al., 2018) and spinal microglia (Ma et al., 2022). DRG macrophages respond to tissue injury and bear a pain-resolving or pain-promoting abilities (Van Der Vlist et al., 2022; Singh et al., 2022; Feng et al., 2023; Yu et al., 2020; Ramin Raoof et al., 2021; Zhang et al., 2016; Liang et al., 2020). Such antinomic/antagonistic functions are not surprising given the phenotypic, spatial and functional heterogeneity of the monocyte/macrophage system (Guilliams et al., 2020, 2018; Guilliams and van de Laar, 2015; Hoeffel and Ginhoux, 2015). This heterogeneity is starting to be appreciated also in DRG tissue (Feng et al., 2023; Lund et al., 2024). Here, we report that lumbar DRG resident macrophages, identified by the expression of CD64 and CX3CR1 markers can be further subdivided into 2 main subsets: SP-macs $CD206^{+}CD163^{-}$ and DP-macs $CD206^{+}CD163^{+}$, which represent respectively 27 and 60 % of total DRG macrophages. Both subsets are long-lived tissue-resident macrophages and exhibit features of perivascular macrophages, in their ability to capture dextran. *In vivo* PLX5622 administration to uninjured animals resulted in a robust depletion of both DRG macrophages subsets, with transient and limited effect on spinal microglia, in spite of the described brain-permeable abilities of PLX5622 (Rebejac et al., 2022; Spangenberg et al., 2019). Interestingly, while SP-macs were rapidly replenished, the numbers of DP-macs remained low over a long-lasting period of time, suggesting differences their turn-over and in their ability to be replenished by circulating monocytes, consistent with recent findings (Lund et al., 2024). Together, these data highlight the potential of DRG resident macrophages to promote pain chronicity, in KO-SGH male mice. This result may appear *a priori* contradictory with previous studies describing $CD206^{+}$ and $CD163^{+}$ macrophages as pain-resolving anti-inflammatory M2 polarized macrophages, in a WT context (Garrity et al., 2023; Niehaus et al., 2021; Van Der Vlist et al., 2022). However, the finding that the DRG resident macrophages are long-lived and that the DP subset occupies the perivascular niche in the DRG fits in a

broader concept arguing for a tissue imprinting of resident macrophages' properties (Gautier et al., 2012; Lavin et al., 2014; Guilliams et al., 2020). It also fits with the idea that DRG macrophages may represent effector cells, bridging the dysbiotic microbiota of KO-SGH males and their predisposition to injury-induced pain. Accordingly, one may hypothesize that given their location in close proximity with the permeable vasculature of DRGs (Harald Lund et al., 2023), the DP subset of DRG macrophages may be first-line targets of circulating microbiota-derived signals. Similar early-life imprinting by the microbiome has been previously reported as affecting gene expression in brain microglia but not yet for other peripheral nervous system-associated macrophages (Thion et al., 2018).

Finally, we also found that female KO-SGH are protected from injury-induced chronic mechanical pain, despite exhibiting a dysbiosis. We further show that despite many similarities in their gut microbiota composition, sex-related differences exist between males and females KO-SGH. Notably, Lactobacillales probiotic species with protective functions, including *Lactobacillus animalis* and *Lactobacillus reuteri* were more abundant in KO-SGH females (Buffington et al., 2016; Chen et al., 2022). In addition, sex differences in pain are increasingly acknowledged, with evidence demonstrating that there are inherent male–female differences in pain processing and modulation (Mogil, 2020). One of the most illustrative examples is the sex-dependent recruitment of the immune system in the settlement of injury-induced pain (Sorge et al., 2015; Guan et al., 2016; Kuhn et al., 2021; Lopes et al., 2017). As male–female differences in the immune system are acknowledged (Klein and Flanagan, 2016), one may speculate that KO-SGH females escape pain chronicity because they recruit a branch of the immune system that may be less affected by the dysbiosis. Accordingly, sex-specific effects of gut microbiota in models of Alzheimer's Disease have been previously reported to be mediated by sex-dependent effect on microglia homeostasis (Dodiya et al., 2019; Thion et al., 2018).

In conclusion, our study extends the current knowledge on the link between a genetically induced dysbiotic gut microbiota and the emergence of injury-induced chronic pain. It also depicts DRG macrophages as effector cells, with a potential to bridge signals from the gut microbiota and the vulnerability to chronic pain. Finally, it underscores sex-specific action of the gut microbiota. Yet, our study bears several limitations, including that: 1) we did not establish whether the dysbiotic microbiota of KO-SGH males is sufficient to promote pain chronicity; 2) mechanistically, we do not show how exactly the genetic Myo1a mutation interacts with gut microbiota in the settlement of chronic pain; 3) we did not establish if a prenatal antibiotic treatment may have similar consequences on the male offspring gut microbiota, in a wild-type context; 4) we cannot completely exclude a possible contribution of SP-DRG macs nor of SC microglia to the chronic pain phenotype of KO-SGH males and 5) we did not decipher how exactly KO-SGH females escape pain chronicity. Further studies are required to address these questions.

In spite of these limitations, the findings presented here reveal the intricate contribution of genes, sex and gut microbiota in determining the vulnerability to chronic somatic pain.

CRediT authorship contribution statement

Ana Reynders: Writing – review & editing, Writing – original draft, Resources, Data curation, Conceptualization. **Z. Anissa Jhumka:** Data generation and curation, Validation, Methodology, Investigation, Conceptualization. **Stéphane Gaillard:** Validation. **Annabelle Mantilleri:** Methodology, Investigation. **Pascale Malapert:** Validation, Methodology. **Karine Magalon:** Validation, Methodology, Data curation. **Anders Etzerodt:** Resources. **Chiara Salio:** Methodology. **Sophie Ugolini:** Resources. **Francis Castets:** Supervision, Methodology, Data curation. **Andrew J. Saurin:** Formal analysis, Data curation. **Matteo Serino:** Methodology, Formal analysis, Data curation. **Guillaume Hoeffel:** Methodology, Validation, Formal Analysis, Data curation. **Aziz Moqrich:** Writing – review & editing, Writing – original draft, Supervision, Project administration, Investigation, Funding acquisition, Conceptualization.

Declaration of competing interest

The authors declare that they have no known competing financial interests or personal relationships that could have appeared to influence the work reported in this paper.

Data availability

Data will be made available on request.

Acknowledgments

We thank all the lab members for their involvement in this project and fruitful discussions.

This project was founded by the French National Agency of Research grants ANR-CE16-Myochronic awarded to AM and ANR-CE16-Floradoloris awarded to AR. It was also supported by funding from CNRS and Aix-Marseille University awarded to IBDM.

Appendix A. Supplementary data

Supplementary data to this article can be found online at https://doi.org/10.1016/j.bbi.2024.05.010.

References

Abraira, V.E., Ginty, D.D., 2013. The sensory neurons of touch. Neuron 79, 618–639. https://doi.org/10.1016/j.neuron.2013.07.051.

Amaral, F.A., Sachs, D., Costa, V.V., Fagundes, C.T., Cisalpino, D., Cunha, T.M., Ferreira, S.H., Cunha, F.Q., Silva, T.A., Nicoli, J.R., Vieira, L.Q., Souza, D.G., Teixeira, M.M., n.d. Commensal microbiota is fundamental for the development of inflammatory pain 5.

Bennett, G.J., Xie, Y.-K., 1988. A peripheral mononeuropathy in rat that produces disorders of pain sensation like those seen in man. PAIN 33.

Boer, C.G., Radjabzadeh, D., Medina-Gomez, C., Garmaeva, S., Schiphof, D., Arp, P., Koet, T., Kurilshikov, A., Fu, J., Ikram, M.A., Bierma-Zeinstra, S., Uitterlinden, A.G., Kraaij, R., Zhernakova, A., van Meurs, J.B.J., 2019. Intestinal microbiome composition and its relation to joint pain and inflammation. Nat Commun 10, 4881. https://doi.org/10.1038/s41467-019-12873-4.

Bonnechère, B., Amin, N., van Duijn, C., 2022. What are the key gut microbiota involved in neurological diseases? A Systematic Review. IJMS 23, 13665. https://doi.org/10.3390/ijms232213665.

Borsook, D., 2012. A future without chronic pain: neuroscience and clinical research. Presented at the Cerebrum: the Dana forum on brain science. Dana Foundation.

Brennan, T.J., 2004. A rat model of postoperative pain. Current protocols. Pharmacology 24. https://doi.org/10.1002/0471141755.ph0534s24.

Brenner, D., Cherry, P., Switzer, T., Butt, I., Stanton, C., Murphy, K., McNamara, B., Iohom, G., O'Mahony, S.M., Shorten, G., 2021. Pain after upper limb surgery under peripheral nerve block is associated with gut microbiome composition and diversity. Neurobiology of Pain 10, 100072. https://doi.org/10.1016/j.ynpai.2021.100072.

Buffington, S.A., Di Prisco, G.V., Auchtung, T.A., Ajami, N.J., Petrosino, J.F., Costa-Mattioli, M., 2016. Microbial reconstitution reverses maternal diet-induced social and synaptic deficits in offspring. Cell 165, 1762–1775. https://doi.org/10.1016/j.cell.2016.06.001.

Chaplan, S.R., Bach, F.W., Pogrel, J.W., Chung, J.M., Yaksh, T.L., 1994. Quantitative assessment of tactile allodynia in the rat paw. J. Neurosci. Methods 53, 55–63. https://doi.org/10.1016/0165-0270(94)90144-9.

Chen, C.-Y., Rao, S.-S., Yue, T., Tan, Y.-J., Yin, H., Chen, L.-J., Luo, M.-J., Wang, Z., Wang, Y.-Y., Hong, C.-G., Qian, Y.-X., He, Z.-H., Liu, J.-H., Yang, F., Huang, F.-Y., Tang, S.-Y., Xie, H., 2022. Glucocorticoid-induced loss of beneficial gut bacterial extracellular vesicles is associated with the pathogenesis of osteonecrosis. Sci. Adv. 8, eabg8335. https://doi.org/10.1126/sciadv.abg8335.

Chen, P., Wang, C., Ren, Y., Ye, Z., Jiang, C., Wu, Z., 2021. Alterations in the gut microbiota and metabolite profiles in the context of neuropathic pain. Mol Brain 14, 50. https://doi.org/10.1186/s13041-021-00765-y.

Clos-Garcia, M., Andrés-Marin, N., Fernández-Eulate, G., Abecia, L., Lavín, J.L., van Liempd, S., Cabrera, D., Royo, F., Valero, A., Errazquin, N., Vega, M.C.G., Govillard, L., Tackett, M.R., Tejada, G., Gónzalez, E., Anguita, J., Bujanda, L., Orcasitas, A.M.C., Aransay, A.M., Maíz, O., López de Munain, A., Falcón-Pérez, J.M., 2019. Gut microbiome and serum metabolome analyses identify molecular biomarkers and altered glutamate metabolism in fibromyalgia. EBioMedicine 46, 499–511. https://doi.org/10.1016/j.ebiom.2019.07.031.

Cobos, E.J., Nickerson, C.A., Gao, F., Chandran, V., Bravo-Caparrós, I., González-Cano, R., Riva, P., Andrews, N.A., Latremoliere, A., Seehus, C.R., Perazzoli, G., Nieto, F.R., Joller, N., Painter, M.W., Ma, C.H.E., Omura, T., Chesler, E.J., Geschwind, D.H., Coppola, G., Rangachari, M., Woolf, C.J., Costigan, M., 2018. Mechanistic differences in neuropathic pain modalities revealed by correlating behavior with global expression profiling. Cell Rep. 22, 1301–1312. https://doi.org/10.1016/j.celrep.2018.01.006.

Cryan, J.F., O'Riordan, K.J., Cowan, C.S.M., Sandhu, K.V., Bastiaanssen, T.F.S., Boehme, M., Codagnone, M.G., Cussotto, S., Fulling, C., Golubeva, A.V., Guzzetta, K. E., Jaggar, M., Long-Smith, C.M., Lyte, J.M., Martin, J.A., Molinero-Perez, A., Moloney, G., Morelli, E., Morillas, E., O'Connor, R., Cruz-Pereira, J.S., Peterson, V.L., Rea, K., Ritz, N.L., Sherwin, E., Spichak, S., Teichman, E.M., van de Wouw, M., Ventura-Silva, A.P., Wallace-Fitzsimons, S.E., Hyland, N., Clarke, G., Dinan, T.G., 2019. The microbiota-gut-brain axis. Physiol. Rev. 99, 1877–2013. https://doi.org/10.1152/physrev.00018.2018.

De Palma, G., Lynch, M.D.J., Lu, J., Dang, V.T., Deng, Y., Jury, J., Umeh, G., Miranda, P. M., Pigrau Pastor, M., Sidani, S., Pinto-Sanchez, M.I., Philip, V., McLean, P.G., Hagelsieb, M.-G., Surette, M.G., Bergonzelli, G.E., Verdu, E.F., Britz-McKibbin, P., Neufeld, J.D., Collins, S.M., Bercik, P., 2017. Transplantation of fecal microbiota from patients with irritable bowel syndrome alters gut function and behavior in recipient mice. Sci. Transl. Med. 9, eaaf6397. https://doi.org/10.1126/scitranslmed.aaf6397.

Delfini, M.-C., Mantilleri, A., Gaillard, S., Hao, J., Reynders, A., Malapert, P., Alonso, S., François, A., Barrere, C., Seal, R., Landry, M., Eschallier, A., Alloui, A., Bourinet, E., Delmas, P., Le Feuvre, Y., Moqrich, A., 2013. TAFA4, a chemokine-like protein, modulates injury-induced mechanical and chemical pain hypersensitivity in mice. Cell Rep. 5, 378–388. https://doi.org/10.1016/j.celrep.2013.09.013.

Ding, W., You, Z., Chen, Q., Yang, L., Doheny, J., Zhou, X., Li, N., Wang, S., Hu, K., Chen, L., Xia, S., Wu, X., Wang, C., Zhang, C., Chen, L., Ritchie, C., Huang, P., Mao, J., Shen, S., 2021. Gut microbiota influences neuropathic pain through modulating proinflammatory and anti-inflammatory T cells. Anesth. Analg. 132, 1146–1155. https://doi.org/10.1213/ANE.0000000000005155.

Dodiya, H.B., Kuntz, T., Shaik, S.M., Baufeld, C., Leibowitz, J., Zhang, X., Gottel, N., Zhang, X., Butovsky, O., Gilbert, J.A., Sisodia, S.S., 2019. Sex-specific effects of microbiome perturbations on cerebral Aβ amyloidosis and microglia phenotypes. J. Exp. Med. 216, 1542–1560. https://doi.org/10.1084/jem.20182386.

Elinav, E., Strowig, T., Kau, A.L., Henao-Mejia, J., Thaiss, C.A., Booth, C.J., Peaper, D.R., Bertin, J., Eisenbarth, S.C., Gordon, J.I., Flavell, R.A., 2011. NLRP6 inflammasome regulates colonic microbial ecology and risk for colitis. Cell 145, 745–757. https://doi.org/10.1016/j.cell.2011.04.022.

Feng, R., Muraleedharan Saraswathy, V., Mokalled, M.H., Cavalli, V., 2023. Self-renewing macrophages in dorsal root ganglia contribute to promote nerve regeneration. Proc. Natl. Acad. Sci. u.s.a. 120 https://doi.org/10.1073/pnas.2215906120.

Finnerup, N.B., Kuner, R., Jensen, T.S., 2021. Neuropathic Pain: From mechanisms to treatment. Physiol. Rev. 101, 259–301. https://doi.org/10.1152/physrev.00045.2019.

Fulde, M., Sommer, F., Chassaing, B., van Vorst, K., Dupont, A., Hensel, M., Basic, M., Klopfleisch, R., Rosenstiel, P., Bleich, A., Bäckhed, F., Gewirtz, A.T., Hornef, M.W., 2018. Neonatal selection by Toll-like receptor 5 influences long-term gut microbiota composition. Nature 560, 489–493. https://doi.org/10.1038/s41586-018-0395-5.

Gaillard, S., Lo Re, L., Mantilleri, A., Hepp, R., Urien, L., Malapert, P., Alonso, S., Deage, M., Kambrun, C., Landry, M., Low, S.A., Alloui, A., Lambolez, B., Scherrer, G., Le Feuvre, Y., Bourinet, E., Moqrich, A., 2014. GINIP, a G αi -interacting protein, functions as a key modulator of peripheral GABA B receptor-mediated analgesia. Neuron 84, 123–136. https://doi.org/10.1016/j.neuron.2014.08.056.

Gangadharan, V., Kuner, R., 2013. Pain hypersensitivity mechanisms at a glance. Dis. Model. Mech. 6, 889–895. https://doi.org/10.1242/dmm.011502.

Garrity, R., Arora, N., Haque, M.A., Weis, D., Trinh, R.T., Neerukonda, S.V., Kumari, S., Cortez, I., Ubogu, E.E., Mahalingam, R., Tavares-Ferreira, D., Price, T.J., Kavelaars, A., Heijnen, C.J., Shepherd, A.J., 2023. Fibroblast-derived PI16 sustains inflammatory pain via regulation of CD206+ myeloid cells. Brain Behav. Immun. 112, 220–234. https://doi.org/10.1016/j.bbi.2023.06.011.

Gautier, E.L., Shay, T., Miller, J., Greter, M., Jakubzick, C., Ivanov, S., Helft, J., Chow, A., Elpek, K.G., Gordonov, S., Mazloom, A.R., Ma'ayan, A., Chua, W.-J., Hansen, T.H., Turley, S.J., Merad, M., Randolph, G.J., Gautier, E.L., Jakubzick, C., Randolph, G.J., Best, A.J., Knell, J., Goldrath, A., Miller, J., Brown, B., Merad, M., Jojic, V., Koller, D., Cohen, N., Brennan, P., Brenner, M., Shay, T., Regev, A., Fletcher, A., Elpek, K., Bellemare-Pelletier, A., Malhotra, D., Turley, S., Jianu, R., Laidlaw, D., Collins, J., Narayan, K., Sylvia, K., Kang, J., Gazit, R., Garrison, B.S., Rossi, D.J., Kim, F., Rao, T. N., Wagers, A., Shinton, S.A., Hardy, R.R., Monach, P., Bezman, N.A., Sun, J.C., Kim, C.C., Lanier, L.L., Heng, T., Kreslavsky, T., Painter, M., Ericson, J., Davis, S., Mathis, D., Benoist, C., the Immunological Genome Consortium, 2012. Gene-expression profiles and transcriptional regulatory pathways that underlie the identity and diversity of mouse tissue macrophages. Nature Immunology 13, 1118–1128. https://doi.org/10.1038/ni.2419.

Gómez-García, A.P., López-Vidal, Y., Pinto-Cardoso, S., Aguirre-García, M.M., 2022. Overexpression of proinflammatory cytokines in dental pulp tissue and distinct bacterial microbiota in carious teeth of Mexican Individuals. Front. Cell. Infect. Microbiol. 12, 958722 https://doi.org/10.3389/fcimb.2022.958722.

Goodrich, J.K., Di Rienzi, S.C., Poole, A.C., Koren, O., Walters, W.A., Caporaso, J.G., Knight, R., Ley, R.E., 2014. Conducting a microbiome study. Cell 158, 250–262. https://doi.org/10.1016/j.cell.2014.06.037.

Guan, Z., Kuhn, J.A., Wang, X., Colquitt, B., Solorzano, C., Vaman, S., Guan, A.K., Evans-Reinsch, Z., Braz, J., Devor, M., Abboud-Werner, S.L., Lanier, L.L., Lomvardas, S., Basbaum, A.I., 2016. Injured sensory neuron–derived CSF1 induces microglial proliferation and DAP12-dependent pain. Nat Neurosci 19, 94–101. https://doi.org/10.1038/nn.4189.

Guilliams, M., Mildner, A., Yona, S., 2018. Developmental and functional heterogeneity of monocytes. Immunity 49, 595–613. https://doi.org/10.1016/j.immuni.2018.10.005.

Guilliams, M., Thierry, G.R., Bonnardel, J., Bajenoff, M., 2020. Establishment and maintenance of the macrophage niche. Immunity 52, 434–451. https://doi.org/10.1016/j.immuni.2020.02.015.

Guilliams, M., van de Laar, L., 2015. A hitchhiker's guide to myeloid cell subsets: Practical implementation of a novel mononuclear phagocyte classification system. Front. Immunol. 6.

Gustafsson, J.K., Ermund, A., Ambort, D., Johansson, M.E.V., Nilsson, H.E., Thorell, K., Hebert, H., Sjövall, H., Hansson, G.C., 2012. Bicarbonate and functional CFTR channel are required for proper mucin secretion and link cystic fibrosis with its mucus phenotype. J. Exp. Med. 209, 1263–1272. https://doi.org/10.1084/jem.20120562.

Hegan, P.S., Kravtsov, D.V., Caputo, C., Egan, M.E., Ameen, N.A., Mooseker, M.S., 2015. Restoration of cytoskeletal and membrane tethering defects but not defects in membrane trafficking in the intestinal brush border of mice lacking both myosin Ia and myosin VI. Cytoskeleton 72, 455–476. https://doi.org/10.1002/cm.21238.

Hoeffel, G., Chen, J., Lavin, Y., Low, D., Almeida, F.F., See, P., Beaudin, A.E., Lum, J., Low, I., Forsberg, E.C., Poidinger, M., Zolezzi, F., Larbi, A., Ng, L.G., Chan, J.K.Y., Greter, M., Becher, B., Samokhvalov, I.M., Merad, M., Ginhoux, F., 2015. C-Myb+ Erythro-myeloid progenitor-derived fetal monocytes give rise to adult tissue-resident macrophages. Immunity 42, 665–678. https://doi.org/10.1016/j.immuni.2015.03.011.

Hoeffel, G., Ginhoux, F., 2015. Ontogeny of tissue-resident macrophages. Front. Immunol. 6.

Hoeffel, G., Debroas, G., Roger, A., Rossignol, R., Gouilly, J., Laprie, C., Chasson, L., Barbon, P.-V., Balsamo, A., Reynders, A., Moqrich, A., Ugolini, S., 2021. Sensory neuron-derived TAFA4 promotes macrophage tissue repair functions. Nature 594, 94–99. https://doi.org/10.1038/s41586-021-03563-7.

Hore, Z., Denk, F., 2019. Neuroimmune interactions in chronic pain – An interdisciplinary perspective. Brain Behav. Immun. 79, 56–62. https://doi.org/10.1016/j.bbi.2019.04.033.

Hulse, R.P., Donaldson, L.F., Wynick, D., 2012. Differential roles of galanin on mechanical and cooling responses at the primary afferent nociceptor. Mol Pain 8. https://doi.org/10.1186/1744-8069-8-41.

Jimenez-Andrade, J.M., Herrera, M.B., Ghilardi, J.R., Vardanyan, M., Melemedjian, O.K., Mantyh, P.W., 2008. Vascularization of the dorsal root ganglia and peripheral nerve of the mouse: Implications for chemical-induced peripheral sensory neuropathies. Mol Pain 4. https://doi.org/10.1186/1744-8069-4-10.

Klein, S.L., Flanagan, K.L., 2016. Sex differences in immune responses. Nat Rev Immunol 16, 626–638. https://doi.org/10.1038/nri.2016.90.

Kravtsov, D.V., Caputo, C., Collaco, A., Hoekstra, N., Egan, M.E., Mooseker, M.S., Ameen, N.A., 2012. Myosin Ia is required for CFTR brush border membrane trafficking and ion transport in the mouse small intestine: Myosin Ia is required for proper CFTR localization. Traffic 13, 1072–1082. https://doi.org/10.1111/j.1600-0854.2012.01368.x.

Kuhn, J.A., Vainchtein, I.D., Braz, J., Hamel, K., Bernstein, M., Craik, V., Dahlgren, M.W., Ortiz-Carpena, J., Molofsky, A.B., Molofsky, A.V., Basbaum, A.I., 2021. Regulatory T-cells inhibit microglia-induced pain hypersensitivity in female mice. Elife 10, e69056.

Lavin, Y., Winter, D., Blecher-Gonen, R., David, E., Keren-Shaul, H., Merad, M., Jung, S., Amit, I., 2014. Tissue-resident macrophage enhancer landscapes are shaped by the local microenvironment. Cell 159, 1312–1326. https://doi.org/10.1016/j.cell.2014.11.018.

Lemire, P., Robertson, S.J., Maughan, H., Tattoli, I., Streutker, C.J., Platnich, J.M., Muruve, D.A., Philpott, D.J., Girardin, S.E., 2017. The NLR protein NLRP6 does not impact gut microbiota composition. Cell Rep. 21, 3653–3661. https://doi.org/10.1016/j.celrep.2017.12.026.

Liang, Z., Hore, Z., Harley, P., Uchenna Stanley, F., Michrowska, A., Dahiya, M., La Russa, F., Jager, S.E., Villa-Hernandez, S., Denk, F., 2020. A transcriptional toolbox for exploring peripheral neuroimmune interactions. Pain 161.

Liao, Y., Smyth, G.K., Shi, W., 2013. The Subread aligner: fast, accurate and scalable read mapping by seed-and-vote. Nucleic Acids Res. 41, e108–e. https://doi.org/10.1093/nar/gkt214.

Liao, Y., Smyth, G.K., Shi, W., 2014. featureCounts: an efficient general purpose program for assigning sequence reads to genomic features. Bioinformatics 30, 923–930. https://doi.org/10.1093/bioinformatics/btt656.

Lopes, D.M., Malek, N., Edye, M., Jager, S.B., McMurray, S., McMahon, S.B., Denk, F., 2017. Sex differences in peripheral not central immune responses to pain-inducing injury. Sci Rep 7, 16460. https://doi.org/10.1038/s41598-017-16664-z.

Love, M.I., Huber, W., Anders, S., 2014. Moderated estimation of fold change and dispersion for RNA-seq data with DESeq2. Genome Biol 15, 550. https://doi.org/10.1186/s13059-014-0550-8.

Luczynski, P., Tramullas, M., Viola, M., Shanahan, F., Clarke, G., O'Mahony, S., Dinan, T. G., Cryan, J.F., 2017. Microbiota regulates visceral pain in the mouse. Elife 6, e25887.

Harald Lund, Matthew Hunt, Zerina Kurtovic, Katalin Sandor, Noah Fereydouni, Anais Julien, Christian Göritz, Jinming Han, Keying Zhu, Robert A. Harris, Jon Lampa, Lisbet Haglund, Tony L. Yaksh, Camilla I. Svensson, 2023. A network of CD163^{+} macrophages monitors enhanced permeability at the blood-dorsal root ganglion barrier. bioRxiv 2023.03.27.534318. https://doi.org/10.1101/2023.03.27.534318.

Lund, H., Hunt, M.A., Kurtović, Z., Sandor, K., Kägy, P.B., Fereydouni, N., Julien, A., Göritz, C., Vazquez-Liebanas, E., Andaloussi Mäe, M., Jurczak, A., Han, J., Zhu, K.,

Harris, R.A., Lampa, J., Graversen, J.H., Etzerodt, A., Haglund, L., Yaksh, T.L., Svensson, C.I., 2024. CD163+ macrophages monitor enhanced permeability at the blood–dorsal root ganglion barrier. J. Exp. Med. 221, e20230675.
Ma, P., Mo, R., Liao, H., Qiu, C., Wu, G., Yang, C., Zhang, Y., Zhao, Y., Song, X.-J., 2022. Gut microbiota depletion by antibiotics ameliorates somatic neuropathic pain induced by nerve injury, chemotherapy, and diabetes in mice. J Neuroinflammation 19, 169. https://doi.org/10.1186/s12974-022-02523-w.
Mamantopoulos, M., Ronchi, F., Van Hauwermeiren, F., Vieira-Silva, S., Yilmaz, B., Martens, L., Saeys, Y., Drexler, S.K., Yazdi, A.S., Raes, J., Lamkanfi, M., McCoy, K.D., Wullaert, A., 2017. Nlrp6- and ASC-dependent inflammasomes do not shape the commensal gut microbiota composition. Immunity 47, 339–348.e4. https://doi.org/10.1016/j.immuni.2017.07.011.
Mazzolini, R., Rodrigues, P., Bazzocco, S., Dopeso, H., Ferreira, A.M., Mateo-Lozano, S., Andretta, E., Woerner, S.M., Alazzouzi, H., Landolfi, S., Hernandez-Losa, J., Macaya, I., Suzuki, H., Ramón y Cajal, S., Mooseker, M.S., Mariadason, J.M., Gebert, J., Hofstra, R.M.W., Reventós, J., Yamamoto, H., Schwartz Jr, S., Arango, D., 2013. Brush border myosin Ia inactivation in gastric but not endometrial tumors. Int. J. Cancer 132, 1790–1799. https://doi.org/10.1002/ijc.27856.
McCafferty, J., Mühlbauer, M., Gharaibeh, R.Z., Arthur, J.C., Perez-Chanona, E., Sha, W., Jobin, C., Fodor, A.A., 2013. Stochastic changes over time and not founder effects drive cage effects in microbial community assembly in a mouse model. ISME J. 7, 2116–2125. https://doi.org/10.1038/ismej.2013.106.
McConnell, R.E., Higginbotham, J.N., Shifrin, D.A., Tabb, D.L., Coffey, R.J., Tyska, M.J., 2009. The enterocyte microvillus is a vesicle-generating organelle. J. Cell Biol. 185, 1285–1298. https://doi.org/10.1083/jcb.200902147.
McConnell, R.E., Tyska, M.J., 2010. Leveraging the membrane – cytoskeleton interface with myosin-1. Trends Cell Biol. 20, 418–426. https://doi.org/10.1016/j.tcb.2010.04.004.
Minerbi, A., Gonzalez, E., Brereton, N.J.B., Anjarkouchian, A., Dewar, K., Fitzcharles, M.-A., Chevalier, S., Shir, Y., 2019. Altered microbiome composition in individuals with fibromyalgia: PAIN 1. https://doi.org/10.1097/j.pain.0000000000001640.
Minerbi, A., Shen, S., 2022. Gut microbiome in anesthesiology and pain medicine. Anesthesiology 137, 93–108. https://doi.org/10.1097/ALN.0000000000004204.
Mogil, J.S., 2020. Qualitative sex differences in pain processing: emerging evidence of a biased literature. Nat Rev Neurosci 21, 353–365. https://doi.org/10.1038/s41583-020-0310-6.
Niehaus, J.K., Taylor-Blake, B., Loo, L., Simon, J.M., Zylka, M.J., 2021. Spinal macrophages resolve nociceptive hypersensitivity after peripheral injury. Neuron 109, 1274–1282.e6. https://doi.org/10.1016/j.neuron.2021.02.018.
O' Mahony, S.M., Dinan, T.G., Cryan, J.F., 2017. The gut microbiota as a key regulator of visceral pain. Pain 158, S19–S28. https://doi.org/10.1097/j.pain.0000000000000779.
Peng, J., Gu, N., Zhou, L., B Eyo, U., Murugan, M., Gan, W.B., Wu, L.J., 2016. Microglia and monocytes synergistically promote the transition from acute to chronic pain after nerve injury. Nat Commun 7, 12029. https://doi.org/10.1038/ncomms12029.
Raoof, R., Gil, C.M., Lafeber, F.P.J.G., de Visser, H., Prado, J., Versteeg, S., Pascha, M.N., Heinemans, A.L.P., Youri Adolfs, R., Pasterkamp, J., Wood, J.N., Mastbergen, S.C., Eijkelkamp, N., 2021. Dorsal root ganglia macrophages maintain osteoarthritis pain. J. Neurosci. 41, 8249. https://doi.org/10.1523/JNEUROSCI.1787-20.2021.
Rebejac, J., Eme-Scolan, E., Arnaud Paroutaud, L., Kharbouche, S., Teleman, M., Spinelli, L., Gallo, E., Roussel-Queval, A., Zarubica, A., Sansoni, A., Bardin, Q., Hoest, P., Michallet, M.-C., Brousse, C., Crozat, K., Manglani, M., Liu, Z., Ginhoux, F., McGavern, D.B., Dalod, M., Malissen, B., Lawrence, T., Rua, R., 2022. Meningeal macrophages protect against viral neuroinfection. Immunity 55, 2103–2117.e10. https://doi.org/10.1016/j.immuni.2022.10.005.
Renthal, W., Tochitsky, I., Yang, L., Cheng, Y.-C., Li, E., Kawaguchi, R., Geschwind, D.H., Woolf, C.J., 2020. Transcriptional reprogramming of distinct peripheral sensory neuron subtypes after axonal injury. Neuron 108, 128–144.e9. https://doi.org/10.1016/j.neuron.2020.07.026.
Reynders, A., Mantilleri, A., Malapert, P., Rialle, S., Nidelet, S., Laffray, S., Beurrier, C., Bourinet, E., Moqrich, A., 2015. Transcriptional profiling of cutaneous MRGPRD free nerve endings and C-LTMRs. Cell Rep. 10, 1007–1019. https://doi.org/10.1016/j.celrep.2015.01.022.
Robertson, S.J., Lemire, P., Maughan, H., Goethel, A., Turpin, W., Bedrani, L., Guttman, D.S., Croitoru, K., Girardin, S.E., Philpott, D.J., 2019. Comparison of Co-housing and littermate methods for microbiota standardization in mouse models. Cell Rep. 27, 1910–1919.e2. https://doi.org/10.1016/j.celrep.2019.04.023.
Segata, N., Izard, J., Waldron, L., Gevers, D., Miropolsky, L., Garrett, W.S., Huttenhower, C., 2011. Metagenomic biomarker discovery and explanation. Genome Biol. 12, R60. https://doi.org/10.1186/gb-2011-12-6-r60.
Serino, M., Luche, E., Gres, S., Baylac, A., Bergé, M., Cenac, C., Waget, A., Klopp, P., Iacovoni, J., Klopp, C., Mariette, J., Bouchez, O., Lluch, J., Ouarné, F., Monsan, P., Valet, P., Roques, C., Amar, J., Bouloumié, A., Théodorou, V., Burcelin, R., 2012. Metabolic adaptation to a high-fat diet is associated with a change in the gut microbiota. Gut 61, 543. https://doi.org/10.1136/gutjnl-2011-301012.
Shen, S., Lim, G., You, Z., Ding, W., Huang, P., Ran, C., Doheny, J., Caravan, P., Tate, S., Hu, K., Kim, H., McCabe, M., Huang, B., Xie, Z., Kwon, D., Chen, L., Mao, J., 2018. Gut Microbiota is critical for the induction of chemotherapy-induced pain 16.
Shi, H., Yin, Z., Koronyo, Y., Fuchs, D.-T., Sheyn, J., Davis, M.R., Wilson, J.W., Margeta, M.A., Pitts, K.M., Herron, S., Ikezu, S., Ikezu, T., Graham, S.L., Gupta, V.K., Black, K.L., Mirzaei, M., Butovsky, O., Koronyo-Hamaoui, M., 2022. Regulating microglial miR-155 transcriptional phenotype alleviates Alzheimer's-induced retinal vasculopathy by limiting Clec7a/Galectin-3+ neurodegenerative microglia. Acta Neuropathol Commun 10, 136. https://doi.org/10.1186/s40478-022-01439-z.
Shifrin, D.A., McConnell, R.E., Nambiar, R., Higginbotham, J.N., Coffey, R.J., Tyska, M.J., 2012. Enterocyte microvillus-derived vesicles detoxify bacterial products and regulate epithelial-microbial interactions. Curr. Biol. 22, 627–631. https://doi.org/10.1016/j.cub.2012.02.022.
Singh, S.K., Krukowski, K., Laumet, G.O., Weis, D., Alexander, J.F., Heijnen, C.J., Kavelaars, A., 2022. CD8+ T cell–derived IL-13 increases macrophage IL-10 to resolve neuropathic pain. JCI Insight 7, e154194.
Sorge, R.E., Mapplebeck, J.C.S., Rosen, S., Beggs, S., Taves, S., Alexander, J.K., Martin, L.J., Austin, J.-S., Sotocinal, S.G., Chen, D., Yang, M., Shi, X.Q., Huang, H., Pillon, N.J., Bilan, P.J., Tu, Y., Klip, A., Ji, R.-R., Zhang, J., Salter, M.W., Mogil, J.S., 2015. Different immune cells mediate mechanical pain hypersensitivity in male and female mice. Nat Neurosci 18, 1081–1083. https://doi.org/10.1038/nn.4053.
Spangenberg, E., Severson, P.L., Hohsfield, L.A., Crapser, J., Zhang, J., Burton, E.A., Zhang, Y., Spevak, W., Lin, J., Phan, N.Y., Habets, G., Rymar, A., Tsang, G., Walters, J., Nespi, M., Singh, P., Broome, S., Ibrahim, P., Zhang, C., Bollag, G., West, B.L., Green, K.N., 2019. Sustained microglial depletion with CSF1R inhibitor impairs parenchymal plaque development in an Alzheimer's disease model. Nat. Commun. 10, 3758. https://doi.org/10.1038/s41467-019-11674-z.
Stappenbeck, T.S., Virgin, H.W., 2016. Accounting for reciprocal host–microbiome interactions in experimental science. Nature 534, 191–199. https://doi.org/10.1038/nature18285.
Stauffer, E.A., Scarborough, J.D., Hirono, M., Miller, E.D., Shah, K., Mercer, J.A., Holt, J.R., Gillespie, P.G., 2005. Fast adaptation in vestibular hair cells requires myosin-1c activity. Neuron 47, 541–553. https://doi.org/10.1016/j.neuron.2005.07.024.
Tap, J., Derrien, M., Törnblom, H., Brazeilles, R., Cools-Portier, S., Doré, J., Störsrud, S., Le Nevé, B., Öhman, L., Simrén, M., 2017. Identification of an intestinal microbiota signature associated with severity of irritable bowel syndrome. Gastroenterology 152, 111–123.e8. https://doi.org/10.1053/j.gastro.2016.09.049.
Thion, M.S., Low, D., Silvin, A., Chen, J., Grisel, P., Schulte-Schrepping, J., Blecher, R., Ulas, T., Squarzoni, P., Hoeffel, G., Coulpier, F., Siopi, E., David, F.S., Scholz, C., Shihui, F., Lum, J., Amoyo, A.A., Larbi, A., Poidinger, M., Buttgereit, A., Lledo, P.-M., Greter, M., Chan, J.K.Y., Amit, I., Beyer, M., Schultze, J.L., Schlitzer, A., Pettersson, S., Ginhoux, F., Garel, S., 2018. Microbiome influences prenatal and adult microglia in a sex-specific manner. Cell 172, 500–516.e16. https://doi.org/10.1016/j.cell.2017.11.042.
Tomas, J., Mulet, C., Saffarian, A., Cavin, J.-B., Ducroc, R., Regnault, B., Kun Tan, C., Duszka, K., Burcelin, R., Wahli, W., Sansonetti, P.J., Pédron, T., 2016. High-fat diet modifies the PPAR-γ pathway leading to disruption of microbial and physiological ecosystem in murine small intestine. Proc. Natl. Acad. Sci. u.s.a. 113 https://doi.org/10.1073/pnas.1612559113.
Tyska, M.J., Mackey, A.T., Huang, J.-D., Copeland, N.G., Jenkins, N.A., Mooseker, M.S., 2005. Myosin-1a Is critical for normal brush border structure and composition. MBoC 16, 2443–2457. https://doi.org/10.1091/mbc.e04-12-1116.
Van Der Vlist, M., Raoof, R., Willemen, H.L.D.M., Prado, J., Versteeg, S., Martin Gil, C., Vos, M., Lokhorst, R.E., Pasterkamp, R.J., Kojima, T., Karasuyama, H., Khoury-Hanold, W., Meyaard, L., Eijkelkamp, N., 2022. Macrophages transfer mitochondria to sensory neurons to resolve inflammatory pain. Neuron 110, 613–626.e9. https://doi.org/10.1016/j.neuron.2021.11.020.
Vannella, K.M., Wynn, T.A., 2017. Mechanisms of organ injury and repair by macrophages. Annu. Rev. Physiol. 79, 593–617. https://doi.org/10.1146/annurev-physiol-022516-034356.
Viennois, E., Pujada, A., Sung, J., Yang, C., Gewirtz, A.T., Chassaing, B., Merlin, D., 2020. Impact of PepT1 deletion on microbiota composition and colitis requires multiple generations. Npj Biofilms Microbiomes 6, 27. https://doi.org/10.1038/s41522-020-0137-y.
Wang, Y., Li, X., Xu, X., Yu, J., Chen, X., Cao, X., Zou, J., Shen, B., Ding, X., 2022. Clec7a expression in inflammatory macrophages orchestrates progression of acute kidney injury. Front. Immunol. 13, 1008727. https://doi.org/10.3389/fimmu.2022.1008727.
Wang, L., Wang, S., Li, W., 2012. RSeQC: quality control of RNA-seq experiments. Bioinformatics 28, 2184–2185. https://doi.org/10.1093/bioinformatics/bts356.
Witschi, R., Punnakkal, P., Paul, J., Walczak, J.-S., Cervero, F., Fritschy, J.-M., Kuner, R., Keist, R., Rudolph, U., Zeilhofer, H.U., 2011. Presynaptic α2-GABA$_A$ receptors in primary afferent depolarization and spinal pain control. J. Neurosci. 31, 8134. https://doi.org/10.1523/JNEUROSCI.6328-10.2011.
Wu, D., Zhang, Y., Zhao, C., Li, Q., Zhang, J., Han, J., Xu, Z., Li, J., Ma, Y., Wang, P., Xu, H., 2022. Disruption of C/EBPβ-Clec7a axis exacerbates neuroinflammatory injury via NLRP3 inflammasome-mediated pyroptosis in experimental neuropathic pain. J Transl Med 20, 583. https://doi.org/10.1186/s12967-022-03779-9.
Xu, Z.-Z., Kim, Y.H., Bang, S., Zhang, Y., Berta, T., Wang, F., Oh, S.B., Ji, R.-R., 2015. Inhibition of mechanical allodynia in neuropathic pain by TLR5-mediated A-fiber blockade. Nat Med 21, 1326–1331. https://doi.org/10.1038/nm.3978.
Yao, Z.-W., Yang, X., Zhao, B.-C., Deng, F., Jiang, Y.-M., Pan, W.-Y., Chen, X.-D., Zhou, B.-W., Zhang, W.-J., Hu, J.-J., Zhu, L., Liu, K.-X., 2022. Predictive and preventive potential of preoperative gut microbiota in chronic postoperative pain in breast cancer survivors. Anesth. Analg. 134.

Yona, S., Kim, K.-W., Wolf, Y., Mildner, A., Varol, D., Breker, M., Strauss-Ayali, D., Viukov, S., Guilliams, M., Misharin, A., Hume, D.A., Perlman, H., Malissen, B., Zelzer, E., Jung, S., 2013. Fate mapping reveals origins and dynamics of monocytes and tissue macrophages under homeostasis. Immunity 38, 79–91. https://doi.org/10.1016/j.immuni.2012.12.001.

Yu, X., Liu, H., Hamel, K.A., Morvan, M.G., Yu, S., Leff, J., Guan, Z., Braz, J.M., Basbaum, A.I., 2020. Dorsal root ganglion macrophages contribute to both the initiation and persistence of neuropathic pain. Nat Commun 11, 264. https://doi.org/10.1038/s41467-019-13839-2.

Zhang, B., Gaiteri, C., Bodea, L.-G., Wang, Z., McElwee, J., Podtelezhnikov, A.A., Zhang, C., Xie, T., Tran, L., Dobrin, R., Fluder, E., Clurman, B., Melquist, S., Narayanan, M., Suver, C., Shah, H., Mahajan, M., Gillis, T., Mysore, J., MacDonald, M.E., Lamb, J.R., Bennett, D.A., Molony, C., Stone, D.J., Gudnason, V., Myers, A.J., Schadt, E.E., Neumann, H., Zhu, J., Emilsson, V., 2013. Integrated systems approach identifies genetic nodes and networks in late-onset alzheimer's disease. Cell 153, 707–720. https://doi.org/10.1016/j.cell.2013.03.030.

Zhang, H., Li, Y., de Carvalho-Barbosa, M., Kavelaars, A., Heijnen, C.J., Albrecht, P.J., Dougherty, P.M., 2016. Dorsal root ganglion infiltration by macrophages contributes to paclitaxel chemotherapy-induced peripheral neuropathy. J. Pain 17, 775–786. https://doi.org/10.1016/j.jpain.2016.02.011.

Zhou, Y., Zhou, B., Pache, L., Chang, M., Khodabakhshi, A.H., Tanaseichuk, O., Benner, C., Chanda, S.K., 2019. Metascape provides a biologist-oriented resource for the analysis of systems-level datasets. Nat Commun 10, 1523. https://doi.org/10.1038/s41467-019-09234-6.

Zimney, K., Van Bogaert, W., Louw, A., 2023. The biology of chronic pain and its implications for pain neuroscience education: State of the art. J. Clin. Med. 12 https://doi.org/10.3390/jcm12134199.